HANDBOOK OF SPIN TRANSPORT AND MAGNETISM

EDITED BY
EVGENY Y. TSYMBAL
IGOR ŽUTIĆ

CRC Press
Taylor & Francis Group
Boca Raton London New York

CRC Press is an imprint of the
Taylor & Francis Group, an **informa** business

IP Bridge Exhibit 2020
Western Digital v. IP Bridge
IPR2024-01494

CRC Press
Taylor & Francis Group
6000 Broken Sound Parkway NW, Suite 300
Boca Raton, FL 33487-2742

© 2012 by Taylor & Francis Group, LLC
CRC Press is an imprint of Taylor & Francis Group, an Informa business

No claim to original U.S. Government works
Version Date: 20110831

International Standard Book Number-13: 978-1-4398-0378-3 (eBook - PDF)

This book contains information obtained from authentic and highly regarded sources. Reasonable efforts have been made to publish reliable data and information, but the author and publisher cannot assume responsibility for the validity of all materials or the consequences of their use. The authors and publishers have attempted to trace the copyright holders of all material reproduced in this publication and apologize to copyright holders if permission to publish in this form has not been obtained. If any copyright material has not been acknowledged please write and let us know so we may rectify in any future reprint.

Except as permitted under U.S. Copyright Law, no part of this book may be reprinted, reproduced, transmitted, or utilized in any form by any electronic, mechanical, or other means, now known or hereafter invented, including photocopying, microfilming, and recording, or in any information storage or retrieval system, without written permission from the publishers.

For permission to photocopy or use material electronically from this work, please access www.copyright.com (http://www.copyright.com/) or contact the Copyright Clearance Center, Inc. (CCC), 222 Rosewood Drive, Danvers, MA 01923, 978-750-8400. CCC is a not-for-profit organization that provides licenses and registration for a variety of users. For organizations that have been granted a photocopy license by the CCC, a separate system of payment has been arranged.

Trademark Notice: Product or corporate names may be trademarks or registered trademarks, and are used only for identification and explanation without intent to infringe.

Visit the Taylor & Francis Web site at
http://www.taylorandfrancis.com

and the CRC Press Web site at
http://www.crcpress.com

Contents

Preface vii
Editors xi
Contributors xiii

PART I Introduction

1 Historical Overview: From Electron Transport in Magnetic Materials to Spintronics 3
Albert Fert

PART II Spin Transport and Magnetism in Magnetic Metallic Multilayers

2 Basics of Nano-Thin Film Magnetism 21
Bretislav Heinrich

3 Micromagnetism as a Prototype for Complexity 47
Anthony S. Arrott

4 Giant Magnetoresistance: Experiment 69
Jack Bass

5 Giant Magnetoresistance: Theory 95
Evgeny Y. Tsymbal, D.G. Pettifor, and Sadamichi Maekawa

6 Spin Injection, Accumulation, and Relaxation in Metals 115
Mark Johnson

7 Spin Torque Effects in Magnetic Systems: Experiment 137
Maxim Tsoi

8 Spin Torque Effects in Magnetic Systems: Theory 157
A. Manchon and Shufeng Zhang

9 Hot Carrier Spin Transport in Ferromagnetic Metals 179
Ron Jansen

PART III Spin Transport and Magnetism in Magnetic Tunnel Junctions

10 Tunneling Magnetoresistance: Experiment (Non-MgO Magnetic Tunnel Junctions) 197
Patrick R. LeClair and Jagadeesh S. Moodera

11 Tunneling Magnetoresistance: Experiment (MgO Magnetic Tunnel Junctions) 217
Shinji Yuasa

12 Tunneling Magnetoresistance: Theory 233
Kirill D. Belashchenko and Evgeny Y. Tsymbal

13 Spin-Filter Tunneling 251
Tiffany S. Santos and Jagadeesh S. Moodera

14 Spin Torques in Magnetic Tunnel Junctions 267
Yoshishige Suzuki and Hitoshi Kubota

15 Multiferroic Tunnel Junctions 285
Manuel Bibes and Agnès Barthélémy

PART IV Spin Transport and Magnetism in Semiconductors

16 Spin Relaxation and Spin Dynamics in Semiconductors 303
Jaroslav Fabian and M.W. Wu

17 Electrical Spin Injection and Transport in Semiconductors 329
Berend T. Jonker

18 Spin-Polarized Ballistic Hot-Electron Injection and Detection in Hybrid Metal–Semiconductor Devices 371
Ian Appelbaum

19 III–V Magnetic Semiconductors 385
Carsten Timm

20 Magnetism of Dilute Oxides 405
J.M.D. Coey

21 Tunneling Magnetoresistance and Spin Transfer with (Ga,Mn)As 427
Henri Jaffrès and Jean-Marie George

22 Spin Transport in Organic Semiconductors 451
Valentin Dediu, Luis E. Hueso, and Ilaria Bergenti

23 Spin Transport in Ferromagnet/III–V Semiconductor Heterostructures 463
Paul A. Crowell and Scott A. Crooker

24 Spin Polarization by Current 487
Sergey D. Ganichev, Maxim Trushin, and John Schliemann

25 Anomalous and Spin-Injection Hall Effects 497
Jairo Sinova, Jörg Wunderlich, and Tomás Jungwirth

PART V Spin Transport and Magnetism at the Nanoscale

26 Spin-Polarized Scanning Tunneling Microscopy 515
Matthias Bode

27 Point Contact Andreev Reflection Spectroscopy 531
Boris E. Nadgorny

28 Ballistic Spin Transport 565
Bernard Doudin and N.T. Kemp

29 Graphene Spintronics 579
Csaba Józsa and Bart J. van Wees

30 Magnetism and Transport in Diluted Magnetic Semiconductor Quantum Dots 599
Joaquín Fernández-Rossier and Ramon Aguado

31 Spin Transport in Hybrid Nanostructures 619
Saburo Takahashi and Sadamichi Maekawa

32 Nonlocal Spin Valves in Metallic Nanostructures 637
Yoshichika Otani and Takashi Kimura

33 Molecular Spintronics 649
Stefano Sanvito

PART VI Applications

34 Magnetoresistive Sensors Based on Magnetic Tunneling Junctions 665
Gang Xiao

35 Magnetoresistive Random Access Memory 685
Johan Åkerman

36 Emerging Spintronics Memories 699
Stuart Parkin, Masamitsu Hayashi, Luc Thomas, Xin Jiang, Rai Moriya, and William Gallagher

37 GMR Spin-Valve Biosensors 715
Drew A. Hall, Richard S. Gaster, and Shan X. Wang

38 Semiconductor Spin-Lasers 731
Igor Žutić, Rafał Oszwałdowski, Jeongsu Lee, and Christian Gøthgen

39 Spin Logic Devices 747
Hanan Dery

Preface

This book addresses two intimately related subjects—spin transport and magnetism. The field of spin transport has emerged from studying the properties of magnetic materials and formed a relatively new research area known as spin electronics, or spintronics. In the past two to three decades, the research on spin transport and magnetism has led to remarkable scientific and technological breakthroughs. A prominent example is the discovery of giant magnetoresistance in magnetic metallic multilayers that was recognized by the 2007 Nobel Prize in Physics awarded to Albert Fert and Peter Grünberg.

The roots of spin transport and spintronics lie in the quantum description of solids, which predicts the existence of the spin, an intrinsic quantity characterizing electrons. The importance of the electron's spin in controlling transport properties was already emphasized by Sir Nevill Mott in 1936 to understand electrical conductivities of the transition metals and their alloys. His two-current model, in which the conductivity is expressed as the sum of two unequal contributions from two different spin projections, explained the high resistivity of ferromagnetic metals relative to their nonmagnetic counterparts. This model introduced the concept of spin transport and showed the importance of magnetism in controlling transport properties. The spin nature of electron transport lies at the heart of modern magnetic data storage technologies, such as computer hard drives and magnetic random access memories (MRAMs). Their operation employs a magnetoresistive device, a metallic spin valve or a magnetic tunnel junction, that consists of two ferromagnetic electrodes separated by a thin spacer layer of nonmagnetic material. The flow of carriers through the device is determined by the direction of their spin relative to the magnetization of the device's electrodes. When the magnetization of the two electrodes is parallel, current flow across the device is permitted; whereas when the magnetization is antiparallel, the current flow is restricted. The corresponding difference in resistance between these two configurations is known as giant magnetoresistance (GMR) if the spacer is metallic and as tunneling magnetoresistance (TMR) if the spacer is insulating.

Early experimental demonstration of Mott's ideas, that the electrical current in magnetic materials is spin polarized, can be inferred from two classes of experiments pertaining to tunneling processes. In 1970, Paul Tedrow and Robert Meservey demonstrated that the tunneling current, originating from a ferromagnetic metal electrode and passing through an insulating alumina barrier, remains spin polarized even outside of the ferromagnetic region. The detection of the spin-polarized current was performed using Zeeman-split density of states in a superconductor, allowing them to quantify the degree of tunneling spin polarization for various ferromagnetic metals. Their studies of the corresponding ferromagnetic/insulator/superconductor junctions have directly guided the discovery of TMR in magnetic tunnel junctions, a key functioning element in modern MRAMs. In 1967, Leo Esaki, Philip Stiles, and Stephan von Molnar employed a metal/magnetic insulator/metal tunnel junction to demonstrate what perhaps can be viewed as the first prototype of a spintronic device. They found that after a large applied bias, the tunneling current depended directly on the magnetization state of the insulator. The height of the insulating barrier layer made of Eu-based chalcogenides could be altered by an applied magnetic field, and the device effectively acted as a spin filter, allowing predominantly the transfer of spins of one direction determined by the magnetization orientation in the insulating film. Doping Eu-chalcogenides with carriers revealed that their ferromagnetic transition temperature can be enhanced, paving a path for versatile magnetic semiconductors that have been intensely studied in the past two decades in which the ferromagnetism may be electrically or optically tuned.

These pioneering contributions to what has subsequently become known as spintronics have foreshadowed the need to study spin transport and magnetism in a wide class of different materials and structures. As this book reveals, some of the key phenomena that were first discovered in one class of materials may have been revisited decades later in other materials systems. A prominent example is the demonstration of spin injection in metals, which, two decades later, was explored in entirely different materials such as silicon, organic semiconductors, carbon nanotubes, and graphene, as well as carefully engineered nanostructures, often with surprising twists and unexpected revelations.

To provide a balanced account of the state-of-the-art standing of the field, we employ a comprehensive approach that covers all the most active research areas in spintronics. Consequently, the content of the book is divided into six parts mostly focusing on

specific materials and structures with extensive cross-references between chapters to reflect the fact that the discoveries in one class of materials may be directly relevant to the breakthroughs in seemingly unrelated systems.

Part I contains a historical and personal perspective of the field written by the Nobel Prize laureate Albert Fert. In addition to his pioneering work on GMR in metallic magnetic multilayers, it contains his first-hand vision of several other topics and materials systems currently actively studied in spintronics.

Part II addresses diverse physical phenomena discovered in hybrid structures of ferromagnetic and normal metals. The part starts from the relevant background in magnetism of magnetic nanostructures where the concepts of magnetic anisotropy, interlayer exchange coupling, exchange bias, and magnetostatic interactions are introduced and discussed. The phenomenon of GMR continues the part. It was discovered that the resistance of a magnetic metallic multilayer drops dramatically when the magnetization alignment of the magnetic layers changes from antiparallel to parallel due to the application of an external magnetic field. A sizable GMR effect persisted at room temperature that opened the way to present-day spintronic applications. Advances in magnetic data storage have enabled nearly a 1000-fold increase in the capacity of computer hard drives using metal-based GMR (and later TMR) spin valves over the last decade. Experiments on electrical spin injection, first envisioned three decades ago, have provided an effective way to generate a nonequilibrium spin population and use it as a sensitive spectroscopic tool to probe fundamental properties such as spin–orbit coupling, spin–Hall effect, hyperfine interactions, and pairing symmetry of unconventional superconductors. Specific nonlocal geometries of lateral spin valves for the spin detection and demonstration of pure spin currents flowing without any accompanying charge currents are now increasingly important in a wide range of materials. The discovery of the spin-torque effect has provided a powerful alternative to the conventional magnetization switching using an external magnetic field, thus offering a wealth of new opportunities for spin transport. Spin-polarized currents interact with ferromagnets, so that a fraction of the spin angular momentum carried by the electrons can be transferred to the ferromagnet. This induces spin-torque-driven magnetic excitations and may be sufficient to reverse the magnetization of the ferromagnet.

Part III is devoted to impressive breakthroughs in spin-dependent tunneling. For more than two decades, after early experiments on spin-dependent tunneling, this area of research has been reserved for only a handful of experts. However, several key developments have dramatically altered this situation. The demonstration of a large and reproducible room temperature TMR in magnetic tunnel junctions in the mid-1990s has shown the practical side of these structures. The latter became especially apparent when a replacement of the amorphous Al_2O_3 tunnel barrier by crystalline MgO led to a more than 10-fold increase in the room temperature TMR. The underlying principle of atomically controlled interfaces for desirable symmetry selection in spin transport, predicted from the first-principles quantum-mechanical calculations, has already led to the development of advanced magnetic fields sensors used in modern hard drives and magnetic data storage elements employed in MRAMs. The tunneling structures are now among the most promising platforms to provide superior spin-based devices and reveal novel fundamental phenomena. For example, using a ferroelectric barrier layer in a magnetic tunnel junction offers a versatile electrical control of TMR through ferroelectric polarization of the barrier.

Traditionally, both spin transport and magnetism have been primarily studied in metallic materials. Part IV reviews the challenges and opportunities for controlling spin and magnetism in semiconductors. Elucidating the underlying mechanisms for spin relaxation and decoherence in semiconductors provides predictive tools to identify the materials and structures that could provide desirably long time- and length-scales for the transfer of spin information. Recent scientific breakthroughs demonstrate that silicon is not only central to conventional electronics, but also offers desirable spin-dependent properties. In silicon, spin can be injected and transferred over more than a millimeter at room temperature. The prospect of silicon spintronics offers an intriguing possibility to combine well-established semiconductor technology with novel spin-related functionalities. Two classes of magnetic semiconductors have been the subject of the intense research effort in the past 15 years. However, the origin of their magnetic ordering remains to be fully understood and continues to be a theoretical challenge. One class is dilute magnetic semiconductors, typically III–V or II–VI compounds doped with Mn of low density. They are remarkably tunable in nature: the ferromagnetic Curie temperature can be controlled externally by light or applied bias. Another class is magnetic oxides, where the ferromagnetic ordering has been reported even in the absence of d-electrons and magnetic impurities. Magnetic semiconductors also offer new possibilities for spin-torque effects, including lower critical currents for magnetization reversal. Spin–orbit coupling arising due to bulk and structure inversion asymmetries is both friend and foe. While often it is desirable to have the spin–orbit coupling reduced, for example, in Si or organic semiconductors to have a longer spin relaxation time, it also is the origin of the fascinating phenomena ranging from the family of spin-dependent Hall effects to generating spin polarization simply by a dc charge current. In addition to the longer-standing tradition of optically injecting and detecting spins in semiconductors, electrical spin injection including related nonlocal effects by now is also well established in semiconductors. Using a tunnel barrier between a ferromagnetic metal and a semiconductor provides robust room temperature spin injection into semiconductors.

Driven by the technological challenge to increase data storage density and enhance the speed of data processing, there is a continuing effort to miniaturize electronic and magnetoresistive devices. A versatile fabrication of various nanostructures can offer favorable scaling properties such as enhanced magnetoresistive effects and room temperature operation otherwise limited to cryogenic temperatures. Part V focuses on the phenomena

characteristic for such nanostructures made of a wide range of materials, including metals, superconductors, molecular magnets, carbon nanotubes, or graphene. Spin-dependent tunneling in nanoscale structures can be used to implement a spin-polarized tunneling microscope that can be used not only to provide atomically resolved information about magnetism, but also to place individual magnetic impurities with atomic-scale precision. Transport measurements, employing Andreev reflection in junctions with a superconducting tip and a ferromagnet, have provided a sensitive probe for the degree of transport spin polarization in a wide range of materials. Spin injection in nanoscale structures can be more pronounced than in their bulk-like counterparts. Efficient magnetization reversal can be implemented using pure spin currents in nonlocal geometries of lateral spin valves while the family of spin-dependent Hall effects can be observed even at room temperature. Semiconductor quantum dots allow for a versatile control of the number of carriers, spin, and the effects of quantum confinement, which leads to improved optical, transport, and magnetic properties as compared to their bulk counterparts. Adding a single carrier in magnetic quantum dots can both strongly change the carrier's spin and the temperature of the magnetization onset.

Part VI addresses the existing and potential spin-based applications that closely rely on the fundamental properties of spin transport and magnetism, discussed in the preceding chapters of the book. This part illustrates methods for improving the operation of metallic spin valves and magnetic tunnel junctions desirable for particular applications and explores paths to novel spin-based applications that are not limited to magnetoresistive effects or conventional metallic structures. The successful use of spin valves and magnetic tunnel junctions is discussed in the chapters devoted to magnetic field sensing and biosensing as well as to nonvolatile MRAMs. A vision for the novel class of spintronic memories explores the possibility to utilize the domain wall motion and implement a three-dimensional integration. Semiconductor spin lasers, in which spin-polarized carriers are injected electrically or optically, have already been demonstrated and have shown advantages over conventional lasers. While the push for ferromagnetic semiconductors has often been motivated by the desire to seamlessly integrate charge-based logic and spin-based information storage, there is also an alternative scheme relying on electrical spin injection in semiconductor/ferromagnetic metal junctions. The envisioned performance in terms of the speed or energy consumption could exceed the ultimate limits possible within conventional electronics.

Overall, this book offers a balanced and thorough treatment of the core principles, theoretical models, experimental approaches, and state-of-the-art applications of spin transport and magnetism, making it suitable for a broad readership. We hope that this book will be an important reference both for graduate students and experienced researchers specializing in the fields of condensed matter physics, materials science, device engineering, and nanoscience.

None of this would have been possible without the dedicated effort of the authors who abandoned, for extended periods of time, their own research to complete their respective chapters, while dealing with the editorial requests for reshaping their style and content. We are thankful to the reviewers who have carefully examined all the chapters and made many helpful suggestions to improve this book. We are also grateful to Verona Skomski for providing invaluable assistance in preparing the book for submission to the publisher. Finally, we acknowledge the support of NSF-DMR, NSF-MRSEC, NSF-ECCS, NSF-EPSCoR, US ONR, AFOSR-DCT, DOE-BES, and SRC, which has enabled our editorial work.

Evgeny Y. Tsymbal
Department of Physics and Astronomy
Nebraska Center for Materials and Nanoscience
University of Nebraska
Lincoln, Nebraska

Igor Žutić
Department of Physics
University at Buffalo
State University of New York
Buffalo, New York

Editors

Evgeny Y. Tsymbal is a Charles Bessey Professor in the Department of Physics and Astronomy at the University of Nebraska-Lincoln (UNL) and the director of the UNL's Materials Research Science and Engineering Center. He joined UNL in 2002 as an associate professor, was promoted to a full professor with tenure in 2005, and named a Charles Bessey Professor of Physics in 2009. Prior to his appointment at UNL, he was a research scientist at the University of Oxford, United Kingdom; a research fellow of the Alexander von Humboldt Foundation at the Research Center-Jülich, Germany; and a research scientist at the Russian Research Center "Kurchatov Institute," Moscow.

Evgeny Tsymbal's research is focused on computational materials science, aiming at the understanding of fundamental properties of advanced ferromagnetic and ferroelectric nanostructures and materials relevant to nanoelectronics and spintronics. He has published over 150 papers, review articles, and book chapters and has presented over 100 invited talks in the areas of spin-dependent transport, magnetoresistive phenomena, nanoscale magnetism, complex oxide heterostructures, interface magnetoelectric phenomena, two-dimensional electron gases, and ferroelectric tunnel junctions. His research has been supported by the National Science Foundation, Semiconductor Research Corporation, the Office of Naval Research, the Department of Energy, Seagate Technology, and the W. M. Keck Foundation.

Evgeny Tsymbal is a fellow of the American Physical Society; a fellow of the Institute of Physics, United Kingdom; and a recipient of the UNL's College of Arts & Sciences Outstanding Research and Creativity Award.

Igor Žutić received his PhD in theoretical physics from the University of Minnesota, after undergraduate studies at the University of Zagreb, Croatia. He was a postdoc at the University of Maryland and the Naval Research Lab. In 2005, he joined the State University of New York at Buffalo as an assistant professor of physics and got promoted to an associate professor in 2009.

Interested to find out if the emerging area of spintronics is only hype or has some future, he proposed and chaired *Spintronics 2001: International Conference on Novel Aspects of Spin-Polarized Transport and Spin Dynamics*, at Washington, DC. The conference appeared to be a success (spintronics was not all hype) and he was invited to write a comprehensive review, Spintronics: Fundamentals and Applications, for the *Reviews of Modern Physics*—currently among the most cited articles on spin transport and magnetism. Work with his collaborators spans a range of topics from high-temperature superconductors and ferromagnetism that can get stronger as the temperature is increased, to prediction of various spin-based devices (some of which were actually realized). He has published over 50 refereed articles and given about 80 invited presentations on spin transport, magnetism, spintronics, and superconductivity.

Igor Žutić is a recipient of the 2006 National Science Foundation CAREER Award, 2005 National Research Council/American Society for Engineering Education Postdoctoral Research Award, and the National Research Council Fellowship (2003–2005). His research is supported by the National Science Foundation, the Office of Naval Research, the Air Force Office of Scientific Research, and the Department of Energy.

Contributors

Ramon Aguado
Department of Teoria y Simulación de Materiales
Instituto de Ciencia de Materiales de Madrid (ICMM), CSIC
Madrid, Spain

Johan Åkerman
Department of Physics
University of Gothenburg
Gothenburg, Sweden

Ian Appelbaum
Department of Physics
University of Maryland
College Park, Maryland

Anthony S. Arrott
Department of Physics
Simon Fraser University
Burnaby, British Columbia, Canada

Agnès Barthélémy
Unité Mixte de Physique
Centre National de la Recherche Scientifique-Thales
Université Paris-Sud
Palaiseau, France

Jack Bass
Department of Physics and Astronomy
Michigan State University
East Lansing, Michigan

Kirill D. Belashchenko
Department of Physics and Astronomy
Nebraska Center for Materials and Nanoscience
University of Nebraska
Lincoln, Nebraska

Ilaria Bergenti
Institute for Nanostructured Materials Studies
Bologna, Italy

Manuel Bibes
Unité Mixte de Physique
Centre National de la Recherche Scientifique-Thales
Université Paris-Sud
Palaiseau, France

Matthias Bode
Department of Physics
University of Würzburg
Würzburg, Germany

J.M.D. Coey
Centre for Research on Adaptive Nanostructures and Nanodevices
School of Physics
Trinity College Dublin
Dublin, Ireland

Scott A. Crooker
National High Magnetic Field Laboratory
Los Alamos National Laboratory
Los Alamos, New Mexico

Paul A. Crowell
School of Physics and Astronomy
University of Minnesota
Minneapolis, Minnesota

Valentin Dediu
Institute for Nanostructured Materials Studies
Bologna, Italy

Hanan Dery
Department of Electrical & Computer Engineering
University of Rochester
Rochester, New York

Bernard Doudin
Institut de Physique et de Chimie des Matériaux de Strasbourg
Centre National de la Recherche Scientifique
University Louis Pasteur
Strasbourg, France

Jaroslav Fabian
Department of Physics
University of Regensburg
Regensburg, Germany

Joaquín Fernández-Rossier
Departamento de Física Aplicada
Universidad de Alicante
Alicante, Spain

Albert Fert
Unité Mixte de Physique
Centre National de la Recherche Scientifique-Thales
Université Paris-Sud
Palaiseau, France

William Gallagher
IBM Thomas J. Watson Research Center
Yorktown Heights, New York

Sergey D. Ganichev
Department of Physics
University of Regensburg
Regensburg, Germany

Richard S. Gaster
Department of Bioengineering
Stanford University
Stanford, California

Jean-Marie George
Unité Mixte de Physique
Centre National de la Recherche Scientifique-Thales
Université Paris-Sud
Palaiseau, France

Christian Gøthgen
Department of Physics
University at Buffalo
State University of New York
Buffalo, New York

Drew A. Hall
Department of Electrical Engineering
Stanford University
Stanford, California

Masamitsu Hayashi
National Institute for Materials Science
Tsukuba, Japan

Bretislav Heinrich
Department of Physics
Simon Fraser University
Burnaby, British Columbia, Canada

Luis E. Hueso
CIC nanoGUNE Consolider
Basque Foundation for Science
Bilbao, Spain

Henri Jaffrès
Unité Mixte de Physique
Centre National de la Recherche Scientifique-Thales
Université Paris-Sud
Palaiseau, France

Ron Jansen
National Institute of Advanced Industrial Science and Technology
Tsukuba, Japan

Xin Jiang
IBM Almaden Research Center
San Jose, California

Mark Johnson
Materials Physics Division
Naval Research Laboratory
Washington, DC

Berend T. Jonker
Magnetoelectronic Materials and Devices Branch
Materials Science and Technology Division
Naval Research Laboratory
Washington, DC

Csaba Józsa
Physics of Nanodevices
Zernike Institute for Advanced Materials
University of Groningen
Groningen, the Netherlands

Tomás Jungwirth
Institute of Physics
Academy of Sciences of the Czech Republic
Prague, Czech Republic

N.T. Kemp
Institut de Physique et de Chimie des Matériaux de Strasbourg
Centre National de la Recherche Scientifique
University Louis Pasteur
Strasbourg, France

Takashi Kimura
Department of Electronic Materials and Devices
INAMORI Frontier Research Center
Kyushu University
Fukuoka, Japan

Hitoshi Kubota
National Institute of Advanced Industrial Science and Technology
Spintronics Research Center
Tsukuba, Japan

Patrick R. LeClair
Department of Physics
and
Astronomy Center for Materials for Information Technology
University of Alabama
Tuscaloosa, Alabama

Jeongsu Lee
Department of Physics
University at Buffalo
State University of New York
Buffalo, New York

Sadamichi Maekawa
Advanced Science Research Center
Japan Atomic Energy Agency
Tokai, Japan

A. Manchon
Department of Physics
University of Arizona
Tucson, Arizona

and

Physical Science and Engineering
King Abdullah University of Science and Technology
Thuwal, Saudi Arabia

Jagadeesh S. Moodera
Francis Bitter Magnet Laboratory
Massachusetts Institute of Technology
Cambridge, Massachusetts

Rai Moriya
Institute of Industrial Science
University of Tokyo
Tokyo, Japan

Boris E. Nadgorny
Department of Physics & Astronomy
Wayne State University
Detroit, Michigan

Rafał Oszwałdowski
Department of Physics
University at Buffalo
State University of New York
Buffalo, New York

Yoshichika Otani
The Institute for Solid State Physics
The University of Tokyo
Chiba, Japan

and

RIKEN ASI Quantum Nano-Scale Magnetics Laboratory
Saitama, Japan

Stuart Parkin
IBM Almaden Research Center
San Jose, California

D.G. Pettifor
Department of Materials
University of Oxford
Oxford, United Kingdom

Tiffany S. Santos
Center for Nanoscale Materials
Argonne National Laboratory
Argonne, Illinois

Stefano Sanvito
Centre for Research on Adaptive Nanostructures and Nanodevices
School of Physics
Trinity College Dublin
Dublin, Ireland

John Schliemann
Department of Physics
University of Regensburg
Regensburg, Germany

Jairo Sinova
Department of Physics
Texas A&M University
College Station, Texas

Yoshishige Suzuki
Department of Materials Engineering Science
Osaka University
Osaka, Japan

Saburo Takahashi
Institute for Materials Research
Tohoku University
Sendai, Japan

Luc Thomas
IBM Almaden Research Center
San Jose, California

Carsten Timm
Institute for Theoretical Physics
Technische Universität Dresden
Dresden, Germany

Maxim Trushin
Department of Physics
University of Regensburg
Regensburg, Germany

Maxim Tsoi
Department of Physics
The University of Texas at Austin
Austin, Texas

Evgeny Y. Tsymbal
Department of Physics and Astronomy
Nebraska Center for Materials and Nanoscience
University of Nebraska
Lincoln, Nebraska

Bart J. van Wees
Physics of Nanodevices
Zernike Institute for Advanced Materials
University of Groningen
Groningen, the Netherlands

Shan X. Wang
Departments of Materials Science and Electrical Engineering
Stanford University
Stanford, California

M.W. Wu
Hefei National Laboratory for Physical Sciences at Microscale
and
Department of Physics
University of Science and Technology of China
Anhui, China

Jörg Wunderlich
Hitachi Cambridge Laboratory
Cambridge, United Kingdom

Gang Xiao
Department of Physics
Brown University
Providence, Rhode Island

Shinji Yuasa
National Institute of Advanced Industrial Science and Technology
Tsukuba, Japan

Shufeng Zhang
Department of Physics
University of Arizona
Tucson, Arizona

Igor Žutić
Department of Physics
University at Buffalo
State University of New York
Buffalo, New York

I

Introduction

1 **Historical Overview: From Electron Transport in Magnetic Materials to Spintronics** *Albert Fert*..... 3
Introduction • Spin-Dependent Conduction in Ferromagnets and Early Examples of Spin Transport Experiments • Concept of GMR in Experiments on Ternary Magnetic Alloys • Discovery of the GMR • Golden Age of GMR • TMR Relays GMR • Spin Accumulation and Spin Currents • Spin Transfer • Spintronics Today and Tomorrow • Conclusion • References

1

Historical Overview: From Electron Transport in Magnetic Materials to Spintronics

1.1 Introduction 3
1.2 Spin-Dependent Conduction in Ferromagnets and Early Examples of Spin Transport Experiments 3
1.3 Concept of GMR in Experiments on Ternary Magnetic Alloys 5
1.4 Discovery of the GMR 6
1.5 Golden Age of GMR 6
1.6 TMR Relays GMR 7
1.7 Spin Accumulation and Spin Currents 9
1.8 Spin Transfer 11
1.9 Spintronics Today and Tomorrow 13
1.10 Conclusion 14
References 15

Albert Fert
Université Paris-Sud

1.1 Introduction

Spintronics is now an important field of research with major applications in several technologies. Its development has been triggered by the discovery [1,2] of the giant magnetoresistance (GMR) in 1988. The basic concept of spintronics is the manipulation of spin-polarized currents, in contrast to mainstream electronics in which the spin of the electron is ignored. Adding the spin degree of freedom provides new effects, new capabilities, and new functionalities. Spin-polarized currents can be generated by exploiting the influence of the spin on the transport properties of the electrons in ferromagnetic conductors. This influence, first suggested by Mott [3], had been experimentally demonstrated and theoretically described in early works [4,5] more than 10 years before the discovery of the GMR. The GMR was the first step on the road of the utilization of the spin degree of freedom in magnetic nanostructures. Its application to the read heads of hard discs greatly contributed to the fast rise in the density of stored information and led to the extension of the hard disk technology to consumer's electronics. Then, the development of an intensive research revealed many other phenomena related to the control and manipulation of spin-polarized currents. Today, the field of spintronics is expanding considerably, with very promising new axes like the manipulation of magnetic moments and the generation of microwaves by spin transfer, spintronics with semiconductors, molecular spintronics, the spin Hall effect (SHE), the quantum spin Hall effect (QSHE), and single-electron spintronics for quantum computing. In this chapter, I will tell the story of this development from the early experiments on spin-dependent conduction in ferromagnets to the emerging directions of today.

1.2 Spin-Dependent Conduction in Ferromagnets and Early Examples of Spin Transport Experiments

GMR and spintronics take their roots in previous researches on the influence of the spin on the electrical conduction in ferromagnetic metals [3–5]. The spin dependence of the conduction can be understood from the typical band structure of a ferromagnetic metal, which is shown in Figure 1.1a. Due to the splitting between the energies of the "majority spin" and "minority spin" directions (spin up and spin down in the usual notation), the electrons at the Fermi level, which carry the electrical current, are in different states and exhibit different conduction properties for opposite spin directions. This spin-dependent conduction was proposed by Mott [3] in 1936 to explain some features of the resistivity of ferromagnetic metals at the Curie temperature. However, in 1966, when I started my PhD thesis, the subject was still almost completely unexplored. My supervisor, Ian Campbell, and I investigated the transport properties of

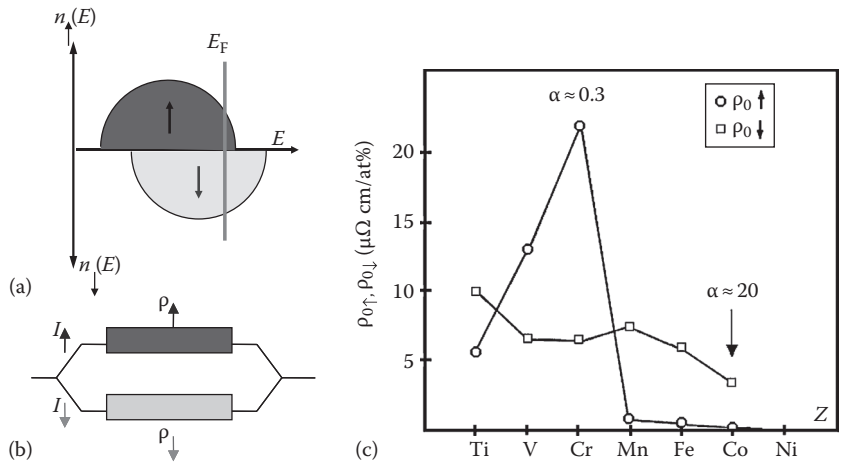

FIGURE 1.1 Basics of spintronics. (a) Schematic band structure of a ferromagnetic metal. (b) Schematic for spin-dependent conduction through independent spin-up and spin-down channels in the limit of negligible spin mixing ($\rho_{\uparrow\downarrow}=0$ in the formalism of Ref. [4]). (c) Resistivities of the spin-up and spin-down conduction channels for nickel doped with 1% of several types of impurity (measurements at 4.2 K) [4]. The ratio α between the resistivities $\rho_{0\downarrow}$ and $\rho_{0\uparrow}$ can be as large as 20 (Co impurities) or, as well, smaller than 1 (Cr or V impurities). (From Fert, A. and Campbell, I.A., *J. Phys. F Met. Phys.*, 6, 849, 1976. With permission.)

Ni- and Fe-based alloys and, from the analysis of the temperature dependence of the resistivity and also from experiments on ternary alloys I describe in Section 1.3, we demonstrated the spin dependence of conduction in various metals and alloys. In particular, we showed that the resistivities of the two channels can be very different in metals doped with impurities presenting a strongly spin-dependent scattering cross-section [4]. In Figure 1.1c, I show the example of the spin-up and spin-down resistivities of nickel doped with 1% of different impurities. It can be seen that the ratio α of the spin-down resistivity to the spin-up one can be as large as 20 for Co impurities or, as well, smaller than the 1 for Cr or V impurities. This was consistent with the theoretical models developed at this time by Jacques Friedel for the electronic structures of impurities in metals. The two-current conduction was rapidly confirmed in other groups and, for example, extended to Co-based alloys by Loegel and Gautier [5].

The so-called two-current model [4] for the conduction in ferromagnetic metals was worked out for the quantitative interpretation of the experiments described in the preceding paragraph. This model is based on a picture of spin-up and spin-down currents coupled by spin mixing, that is, by exchange of current between the spin-up and spin-down channels. Spin mixing comes from spin-flip scattering, mainly from electron-magnon scattering, which conserves the total spin of the electronic system but is a mechanism of current transfer between the two channels. It increases with temperature and tends to equalize partly the spin-up and spin-down currents at room temperature in most ferromagnetic metals [4]. The two-current model is the basis of spintronics today, but, except in very few publications [6,7] discussing the temperature dependence of the GMR, the interpretation of the spintronics phenomena is surprisingly based on a simplified version of the model neglecting spin mixing and assuming that the conduction is by two independent channels in parallel, as in the sketch of Figure 1.1c. It should be certainly useful to revisit the interpretation of many recent experiments by taking into account the spin mixing contributions (note that the spin mixing mechanism by spin-flips should not be confused with the spin relaxation mechanism transferring spin accumulation to the lattice and due mainly to spin–orbit scattering).

The research on spin transport developed before the discovery of GMR has not only worked out the basic physics of spin transport in ferromagnetic conductors but also explored some topics that came into fashion only recently in spintronics. I take the example of the SHE. When an electrical current flows in a nonmagnetic conductor, the electrons of opposite spins are deflected to opposite transverse directions by spin–orbit interactions. With equal spin-up and spin-down currents, there is no charge accumulation and consequently no Hall voltage between edge contacts, but the deflections induce opposite spin accumulations on the edges of the conductor, as illustrated in Figure 1.2a. This is the SHE, already described in 1971 by D'yakonov and Perel' [8].

As the spin accumulation by SHE can be used to generate spin currents, the SHE is nowadays presented as a possible way for spintronics without magnetic materials, which explains the intense current research on the topic. In most experiments of the recent years, the SHE is detected by breaking the symmetry between the opposite spin directions to obtain a transverse voltage, either by using a ferromagnetic metal for one of the Hall probes or by injecting locally a spin-polarized current (or even a pure spin current) from a ferromagnetic contact, the so-called inverse SHE detection. This can be done only in nano-devices fabricated by lithographic techniques [9–11]. Thirty years ago, it was not technically possible to fabricate such nano-devices,

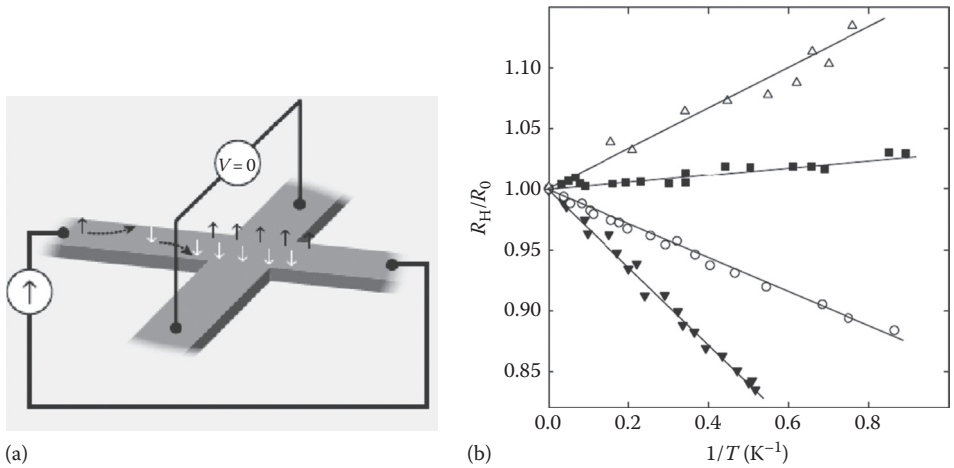

FIGURE 1.2 (a) Sketch illustrating the SHE in a nonmagnetic conductor. (b) Experimental results [12] on the SHE induced by resonant scattering on 5d levels (split by spin–orbit coupling) of nonmagnetic impurities in Cu (open triangles = Lu 0.013%, circles = Ta 0.023%, black triangle = Ir 0.19%). The inverse SHE of the Cu alloys is revealed by adding ≈ 0.01% of Mn impurities and applying a field H to spin-polarize the current by exchange scattering on the spin-polarized Mn impurities. With a paramagnetic-like spin polarization proportional to H/T, the SHE is revealed by a contribution to the Hall constant proportional to T^{-1} with different slopes for different impurities (the squares represent measurement on Cu with only 0.015% of Mn and without 5d impurities, which shows the quasi-absence of $1/T$ contribution to the Hall effect from Mn alone). Note the characteristic change of sign of the SHE between the beginning (Lu) and the end (Ir) of the 5d series.

but, nevertheless, a precise determination of the SHE could be performed in other ways. In Figure 1.2b, we show the results published in 1981 [12] on the SHE induced by 5d impurities (Lu, Ta, Ir, Au) in Cu. The SHE is detected by adding 0.01% of Mn impurities and applying a magnetic field. It had previously been shown that applying a field with only Mn impurities in Cu does not give any significant contribution to the Hall effect but induces (by exchange scattering) a spin polarization of the current, which can be known from the associated negative magnetoresistance (GMR-like effect). In brief, the spin polarization induced by exchange with dilute impurities of Mn replaces the spin injection of modern experiments. As the current polarization follows the polarization of the paramagnetic Mn impurities and is inversely proportional to the temperature (T), one obtains the variations of the Hall constant as $1/T$ seen in Figure 1.2b for different types of nonmagnetic impurities. The amplitude of the SHE can be characterized by the Hall angle, $\Phi_H = \rho_{xy}/\rho_{xx}$. From the results of Figure 1.2b, Fert et al. [12] have derived Hall angles varying from -2.4×10^{-2} for CuLu to $+5.2 \times 10^{-2}$ for CuIr, with the typical change of sign between the beginning and the end of the 5d series predicted by a model of resonant scattering on impurity 5d states split by spin–orbit interaction (–1.2% and +2.6% if we divide by 2 to take into account the different definition of the Hall angle today).

The mechanism of resonant skew scattering by impurity levels explains that the SHE Hall angle in Ref. [12] is larger by one or two orders of magnitude than that found in modern experiments for most pure metals [9–11] or semiconductors [13]. Actually a larger angle was recently reported for Au spin-injected from FePt [11], but more recent experiments in the same group seem to show this large SHE comes from Pt impurities and probably from the same mechanism as in the alloys of Figure 1.2b.

1.3 Concept of GMR in Experiments on Ternary Magnetic Alloys

Twenty years before the discovery of GMR, some experiments with ferromagnetic metals doped with two types of impurities [4] were already anticipating the GMR. This is illustrated in Figure 1.3. Suppose, for example, that nickel is doped with impurities A (Co, for example), which scatter strongly the electrons of the spin-down channel and with impurities B (Rh, for example), which scatter strongly the spin-up electrons. In the ternary alloy Ni(Co + Rh), that I call of type 1, the electrons of both channels are strongly scattered either by Co in one of the channels or by Rh in the other, so that there is no shorting by one of the channels and the resistivity is strongly enhanced, as illustrated in Figure 1.3a. In contrast, there is no such enhancement in alloys of type 2 doped with impurities A and B (Co and Au, for example) scattering strongly the electrons in the same channel and leaving the second channel open, as in Figure 1.3b.

The idea of GMR is the replacement of the impurities A and B of the ternary alloy by the successive layers A and B of the same magnetic metal in a multilayer. If the magnetizations of the layers A and B are antiparallel, this corresponds to the situation of strong scattering in both channels in alloys of type 1, while the configuration with parallel magnetizations corresponds to the situation with a relatively free channel in alloys of type 2. What is new with respect to the ternary alloys is the possibility of switching between high and low resistivity states applying a magnetic field and by simply changing the relative orientation of the magnetizations of layers A and B from antiparallel to parallel. However, the transport equations tell us that the relative

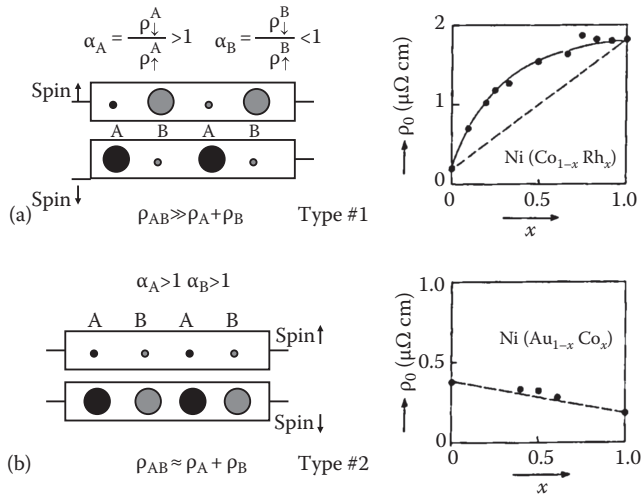

FIGURE 1.3 Experiments on ternary alloys based on the same concept as that of the GMR [4]. On the sketches illustrating the conduction by two channels in a ferromagnet doped with impurities A (black) and B (grey), the circles are at the scale of the scattering cross-sections of impurities A and B. (a) Schematic for the spin-dependent conduction in alloys with impurities of opposite scattering spin asymmetries ($\alpha_A = \rho_{A\downarrow}/\rho_{A\uparrow} > 1$, $\alpha_B = \rho_{B\downarrow}/\rho_{B\uparrow} < 1$, $\rho_{AB} \gg \rho_A + \rho_B$) and experimental results for $Ni(Co_{1-x}Rh_x)$ alloys. (b) Same for alloys with impurities of similar scattering spin asymmetries ($\alpha_A = \rho_{A\downarrow}/\rho_{A\uparrow} > 1$, $\alpha_B = \rho_{B\downarrow}/\rho_{B\uparrow} > 1$, $\rho_{AB} \approx \rho_A + \rho_B$) and experimental results for $Ni(Au_{1-x}Co_x)$ alloys. In GMR, the impurities A and B are replaced by multilayers, the situation of (a) corresponding to the antiparallel magnetic configurations of adjacent magnetic layers and (b) corresponding to parallel.

orientation of layers A and B can be felt by the electrons only if their distance is smaller than the electron mean free path, that is, practically, if they are spaced by only a few nanometers. Unfortunately, in the 1970s, it was not technically possible to make multilayers with layers as thin as a few nanometers, and the discovery of the GMR waited until the development of sophisticated deposition techniques.

1.4 Discovery of the GMR

In the mid-1980s, with the development of techniques like the molecular beam epitaxy (MBE), it became possible to fabricate multilayers composed of very thin individual layers and one could consider trying to extend the experiments on ternary alloys to multilayers. In addition, in 1986, I saw the beautiful Brillouin scattering experiments of Grünberg and coworkers [14] revealing the existence of antiferromagnetic interlayer exchange couplings in Fe/Cr multilayers. Fe/Cr appeared as a magnetic multilayered system in which it was possible to switch the relative orientation of the magnetization in adjacent magnetic layers from antiparallel to parallel by applying a magnetic field. In collaboration with the group of Alain Friederich at the Thomson-CSF company, I started the fabrication and investigation of Fe/Cr multilayers. This led us in 1988 to the discovery [1] of very large magnetoresistance effects that we called GMR (Figure 1.4a). Effects of the same type in Fe/Cr/Fe trilayers were obtained practically at the same time by Grünberg at Jülich [2] (Figure 1.4b). The interpretation of the GMR is similar to that described above for the ternary alloys and is illustrated in Figure 1.4c. The first classical model of the GMR was published in 1989 by Camley and Barnas [15], and I collaborated with Levy and Zhang for the first quantum model [16] in 1991.

I am often asked if I was expecting such large MR effects. My answer is yes and no: on one hand, a very large magnetoresistance could be expected from an extrapolation of the preceding results on ternary alloys, on the other hand one could fear that the unavoidable structural defects of the multilayers, interface roughness, for example, might introduce spin-independent scatterings canceling the spin-dependent scattering inside the magnetic layers. The good luck was finally that the scattering by the roughness of the interfaces is also spin dependent and adds its contribution to the "bulk" one (the "bulk" and interface contributions can be separately derived from GMR experiments with the current perpendicular to the layers).

1.5 Golden Age of GMR

Rapidly, the papers reporting the discovery of GMR attracted attention for their fundamental interest as well as for the many possibilities of applications, and the research on magnetic multilayers and GMR became a very hot topic. In my team, as well as in the small but rapidly increasing community working in the field, we had the exalting impression of exploring a wide virgin country with so many amazing surprises in store. On the experimental side, two important results were published in 1990. Parkin et al. [17] demonstrated the existence of GMR in multilayers made by the simpler and faster technique of sputtering (Fe/Cr, Co/Ru, and Co/Cr) and found the oscillatory behavior of the GMR due to the oscillations of the interlayer exchange as a function of the thickness of the nonmagnetic layers (see Figure 1.5). Also in 1990, Shinjo and Yamamoto [18], as well as Dupas et al. [19], demonstrated that GMR effects can be found in multilayers without antiferromagnetic interlayer coupling but composed of magnetic layers of different coercivities. Another important result, in 1991, was the observation of large and oscillatory GMR effects in Co/Cu, which became an archetypical GMR system. The first observations were obtained at Orsay [20] with multilayers prepared by sputtering at Michigan State University and at about the same time at IBM [21].

Also in 1991, Dieny et al. [22] reported the first observation of GMR in spin-valves, that is, trilayered structures in which the magnetization of one of the two magnetic layers is pinned by coupling with an antiferromagnetic layer while the magnetization of the second one is free. The magnetization of the free layer can be reversed by very small magnetic fields, so that the concept is now used in many devices. The various applications of the GMR are described in other chapters of the book. Its application to the read heads of the hard discs is certainly the most important [23,24]. The GMR, by providing a sensitive and scalable read technique, has led to an increase of the areal recording density by more than two orders of magnitude (from ≈1 to ≈600 Gbit/in.^{2}

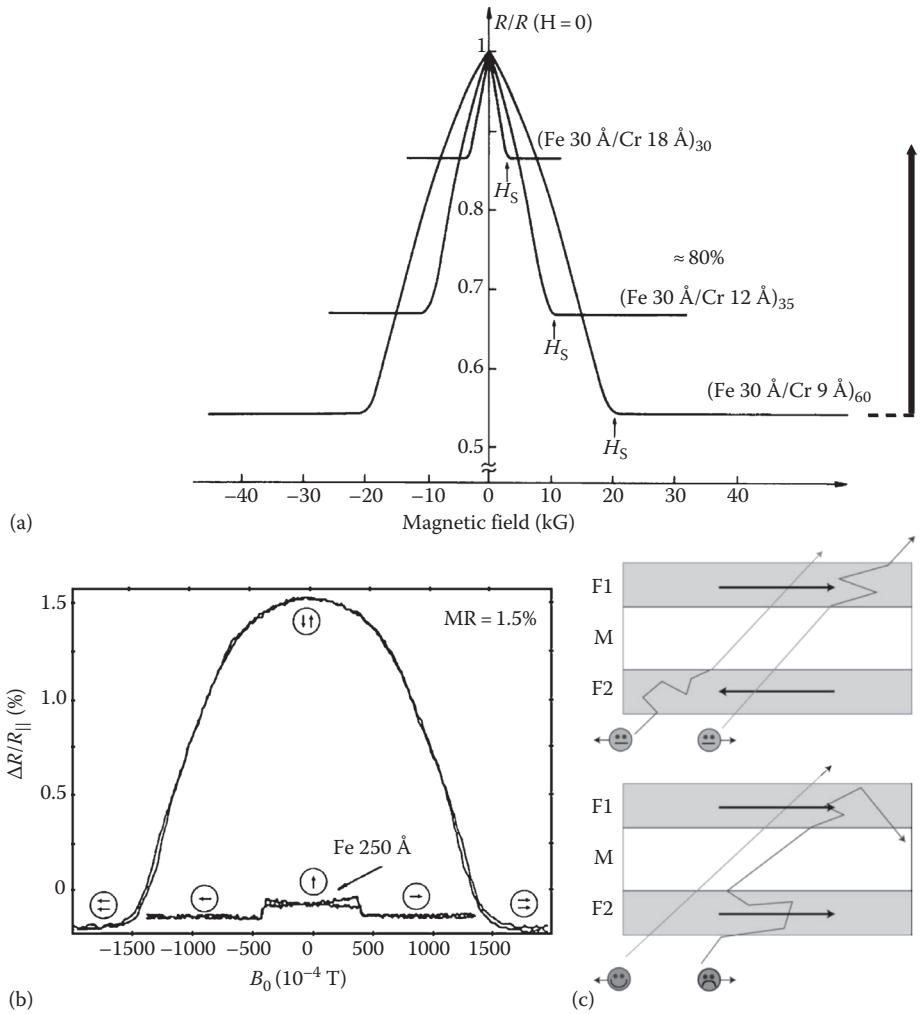

FIGURE 1.4 First observations of giant magnetoresistance. (a) Fe/Cr(001) multilayers [1] (with the current definition of the magnetoresistance ratio, MR= $100[R_{AP}-R_P]/R_p$, MR = 85% for the Fe 3 nm/Cr 0.9 nm multilayer). (b) Fe/Cr/Fe trilayers [2]. (c) Schematic of the mechanism of the GMR. In the parallel magnetic configuration (bottom), the electrons of one of the spin directions can go easily through all the magnetic layers and the short circuit through this channel leads to a small resistance. In the antiparallel configuration (top), the electrons of each channel are slowed down every second magnetic layer and the resistance is high. (From Chappert, C. et al., *Nat. Mater.*, 6, 813, 2007. With permission.)

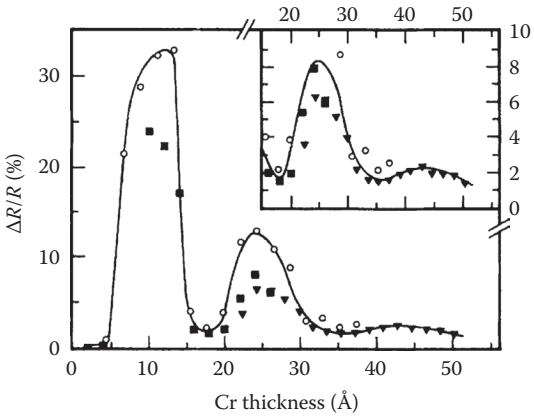

FIGURE 1.5 Oscillatory variation of the GMR ratio of Fe/Cr multilayers as a function of the thickness of the Cr layers. (From Parkin, S.S.P. et al., *Phys. Rev. Lett.*, 64, 2304, 1990. With permission.)

in 2009). This increase opened the way both to unprecedented drive capacities (up to 1 terabyte) for video recording or backup and to smaller hard disc drive (HDD) sizes (down to .85 in. disk diameter) for mobile appliances like ultra-light laptops or portable multimedia players. GMR sensors are also used in many other types of application, mainly in automotive industry and biomedical technology [25].

1.6 TMR Relays GMR

An important stage in the development of spintronics has been the research on the tunneling magnetoresistance (TMR) of the magnetic tunnel junctions (MTJs). The MTJs are tunnel junctions with ferromagnetic electrodes, and their resistance is different for the parallel and antiparallel magnetic configurations of their electrodes. Some early observations of small TMR effects had been already reported by Jullière [26] in 1975 and Maekawa

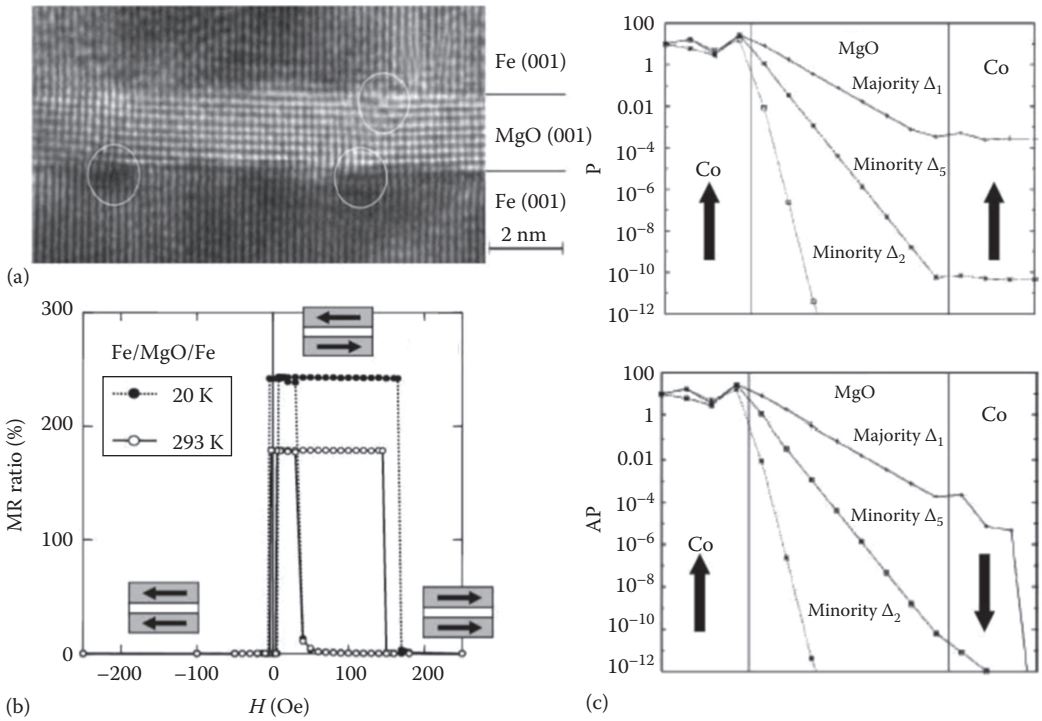

FIGURE 1.6 TMR of MTJ with MgO barrier. (a) Electron microscopy image of an Fe(001)/MgO(001)/Fe(001) MTJ [30]. (b) MR = $(R_{max} - R_{min})/R_{min}$ measured by Yuasa et al. [30] for a Fe(001)/MgO(001)/Fe(001) MTJ. (c) Physics of the TMR illustrated by the decay of evanescent electronic waves of different symmetries in an MgO(001) layer between cobalt electrodes calculated by Zhang and Butler [37]. The Δ_1 symmetry of the slowly decay tunneling channel is well represented at the Fermi level of the spin conduction band of cobalt for the majority spin direction and not for the minority spin one, so that a spin conserving connection through the channel Δ_1 is possible in the parallel configuration. This explains the very high TMR of this type of junction.

and Gäfvert [27] in 1982, but they were found to be hardly reproducible and actually could not be really reproduced until 1995. It was at this time only that large (≈20%) and reproducible effects were obtained by Moodera's and Miyasaki's groups on MTJ with a tunnel barrier of amorphous alumina [28].

After 1995, the research on TMR became very active, and the most important step was the transition from MTJ with amorphous tunnel barrier (alumina) to single-crystal MTJ and especially MTJ with MgO barrier. In the first results with MgO, the TMR ratio was only slightly larger than that found with alumina barriers and similar electrodes [29]. The important breakthrough came in 2004 at Tsukuba [30] and IBM [31] where it was found that very large TMR ratios, up to 200% at room temperature, could be obtained with MgO MTJ of very high structural quality, as illustrated in Figure 1.6. Since 2004, these results have been progressively improved [32], and TMR ratios up to 1000% have been now reached [33].

The large TMR of MTJ with single-crystal tunnel barriers like MgO(001) comes from symmetry selection [34–37]. This is illustrated in Figure 1.6c where one sees the calculated density of states (DOS) of evanescent wave functions of different symmetries, Δ_1, Δ_5, etc., and the much slower decay of the symmetry Δ_1 in a MgO(001) barrier between Co electrodes [37]. The key point is that, at least for interfaces of high quality, an evanescent wave function of a given symmetry is connected to the Bloch functions of the same symmetry and same spin direction at the Fermi level of the electrodes. For Co electrodes, the Δ_1 symmetry is well represented at the Fermi level in the majority spin direction sub-band and not in the minority one. Consequently, a good connection between the majority spin direction sub-bands of the Co electrodes by the slowly decaying channel Δ_1 can be obtained only in their parallel magnetic configuration, which explains the very high TMR. Other types of barriers can select symmetries other than the symmetry Δ_1 selected by MgO(001). For example, an $SrTiO_3$ barrier predominantly selects evanescent wave functions of Δ_5 symmetry, which are well connected to minority spin states of cobalt [38]. This explains the negative effective spin polarization of cobalt observed in $SrTiO_3$-based MTJ [39].

The high spin polarization obtained by symmetry selection gives a very good illustration of what is under the word "spin polarization" in a spintronic experiment. There is no intrinsic spin polarization of a magnetic conductor. In an MTJ, the effective polarization is related to the symmetry selected by the barrier and, depending on the barrier, can be positive or negative, large or small. In the same way, as we have seen in Section 1.2, the spin polarization of metallic conduction depends strongly on the spin dependence of the scattering by impurities, as shown in Figure 1.1b.

The MTJ with MgO barrier are today the most efficient "spin polarizers" and are used in many experiments and devices.

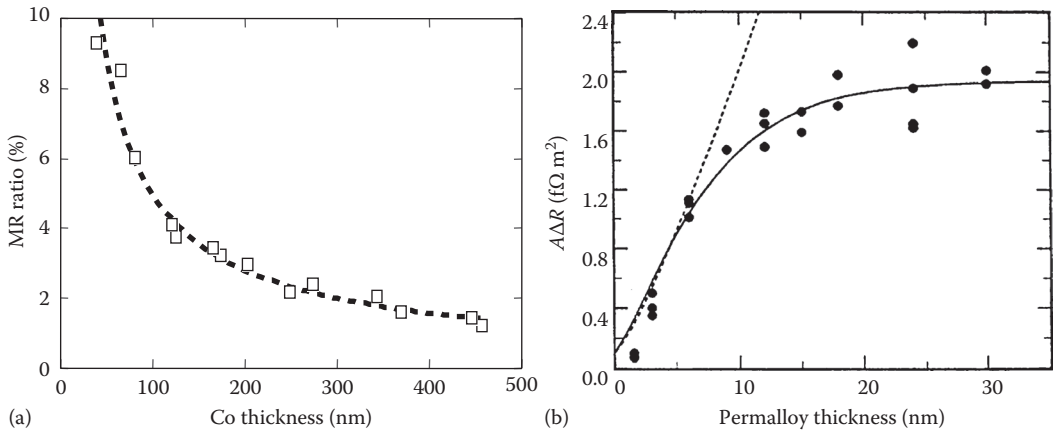

FIGURE 1.7 Experimental results illustrating the thickness dependence of the CPP-GMR and its relation with the SDL. (a) CPP-GMR of Co/Cu/Co multilayers electrodeposited into pores of membranes [44]. With the long SDL of Co (60 nm), the GMR can be seen up to Co thicknesses in the μm range. (b) CPP-GMR of Py/Cu/Py multilayers [43]. With an SDL of only 5 nm, the resistance change between P and AP configuration flattens out, for permalloy layers thicker than 10 nm and, as the resistance still increase, the GMR ratio decreases to zero.

However, other directions are also explored to obtain even larger TMR. One of these directions is the research of half-metallic materials, in other words materials of metallic character for one of the spin directions and insulating for the other, which means a 100% polarization. Some oxides and Heusler alloys close to half-metallicity have been found [40,41]. Spin filtering by a ferromagnetic barrier is another interesting concept [42].

From a technological point of view, the interest of the MTJ with respect to the metallic spin valves comes from the vertical direction of the current and from the resulting possibility of a reduction of the lateral size to a submicronic scale by lithographic techniques. The MTJs are at the basis of a new concept of magnetic memory called magnetic random access memory (MRAM), which is expected to combine the short access time of the semiconductor-based RAMs and the nonvolatile character of the magnetic memories [24]. In the first MRAMs, put onto the market in 2006, the memory cells are MTJs with an alumina barrier. The magnetic fields generated by "word" and "bit" lines are used to switch their magnetic configuration. The next generation of MRAM, based on MgO tunnel junctions and switching by spin transfer, is expected to have a much stronger impact on the technology of the computers.

1.7 Spin Accumulation and Spin Currents

During the first years of the research on GMR, the experiments were performed only with currents flowing along the layer planes—in the geometry called CIP (current in plane). It is only in 1991 that experiments of GMR with the current perpendicular to the layer planes (CPP-GMR) begun to be performed. This was done first by sandwiching a magnetic multilayer between superconducting electrodes [43], then by electrodepositing multilayers into the pores of a polycarbonate membrane [44], and, more recently, in vertical nanostructures fabricated by e-beam lithographic techniques (pillars). In the CPP geometry, the GMR not only is definitely higher than that in CIP but also subsists in multilayers with relatively thick layers, up to the micron range in Figure 1.7a, for example. The Valet–Fert model [45] explains that, owing to spin accumulation effects occurring in the diffusive regime of transport, the length scale of the CPP-GMR becomes the long spin diffusion length (SDL) in place of the short mean free path for the CIP geometry.

Actually, the CPP-GMR revealed clearly the spin accumulation effects, which govern the propagation of a spin-polarized current through a succession of magnetic and nonmagnetic materials and play an important role in all the current developments of spintronics. The diffusion current induced by the accumulation of spins at the magnetic/nonmagnetic interface is the mechanism driving a spin-polarized current in a nonmagnetic conductor to a long distance from the interface, well beyond the ballistic range (i.e., well beyond the mean free path) up to the distance of the SDL. In carbon molecules, for example, the SDL exceeds largely the micron range and, as we see in Section 1.11, strongly spin-polarized currents can be transported throughout long carbon nanotubes (CNTs) [46].

The physics of the spin accumulation occurring when an electron flux crosses an interface between a ferromagnetic and a nonmagnetic material is explained in Figure 1.8 for a simple situation (single interface, no interface resistance, no band bending, and single polarity). To sum up, there is a broad zone of spin accumulation, which extends on both sides of an F/N interface and in which the spin polarization of the injected current subsists in N to a distance of the order of the SDL (or start at this distance for the opposite current direction). The spin polarization just at the interface depends on the proportion of the depolarizing (polarizing) spin-flips induced by the spin accumulation in F and N. If the DOS and the spin relaxation times are similar on both sides, there is a balanced proportion of spin-flips on the N and F sides, and the current is significantly spin-polarized in

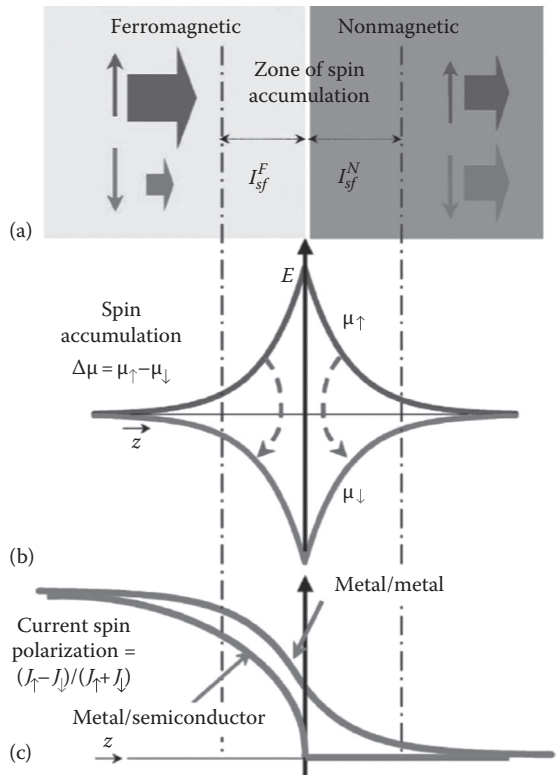

FIGURE 1.8 (See color insert.) Schematic representation of the spin accumulation at an interface between a ferromagnetic metal and a nonmagnetic layer. (a) Incoming and outgoing spin-up and spin-down currents. (b) Splitting of the chemical potentials, $E_{F\uparrow}$ and $E_{F\downarrow}$, in the interface region with arrows symbolizing the spin-flips induced by the spin accumulation (out of equilibrium distribution), spin-flips controlling the progressive depolarization of the current. With an opposite direction of the current, the inversion of the spin accumulation and the opposite spin-flips polarize progressively the current. (c) Variation of the current spin polarization when there is an approximate balance between the spin-flips on both sides (metal/metal curve) and when the spin-flips on the right side are predominant (metal/semiconductor curve in the situation without spin-dependent interface resistance). (From Chappert, C. et al., *Nat. Mater.*, 6, 813, 2007. With permission.)

N (as for the metal/metal curve in Figure 1.8c). In contrast, if the DOS is much smaller or the spin relaxation time much shorter in N, the depolarization (or polarization for spin extraction) occurs mainly in F and the current is negligibly spin-polarized in N. This corresponds to the situation for the metal/semiconductor curve in Figure 1.8c. This difficulty when F is a metal and N a semiconductor has been first described by Schmidt et al. [47] and called "conductivity mismatch." The problem can be solved by inserting a spin-dependent interface resistance (tunnel junction) to induce a discontinuity of the spin accumulation, which increases the Fermi energy spitting and the proportion of spin-flips on the side N of the interface [48,49].

The physics of spin accumulation and spin-polarized currents, which plays an important role in most fields of spintronics today, can be described by new types of transport equation [45,49,50], often called drift/diffusion equations, in which the electrical potential is replaced by a spin- and position-dependent electrochemical potential. These equations can also be extended to take into account band bending and high current density effects [51]. They have been frequently applied to the general situation of multi-contact systems with interplay of the spin accumulation effects at different contacts [49,52,53]. A standard structure is a nonmagnetic lateral channel, metal, semiconductor, or carbon-based conductor, between a spin-polarized source F1 and a spin-polarized drain F2. The output "spin signal" is the resistance or voltage difference between different magnetic configurations of the contacts. Very generally, one distinguishes local geometries in which the output signal is measured between the source and the drain (Figure 1.9a), and nonlocal geometries in which the output signal is between two other contacts (Figure 1.9b). In the nonlocal geometry of Figure 1.9b, where the current flows to the left with a spin accumulation spreading to the right (Figure 1.9c), the output voltage V reflects the spin accumulation splitting at the magnetic contact F2 and is inverted when one reverses the magnetization of F2. Note that, in the right part of the channel, the opposite gradients of spin-up and spin-down chemical potentials generate opposite spin-up and spin-down currents, or, in other words, a pure spin current without charge current.

In Figure 1.9e, we show an example of the application of the drift-diffusion equations to the problem of spin transport in a nonmagnetic lateral channel between spin-polarized source and drains connected to the channel by a spin-dependent interface resistance (MTJ, for example). The calculation is performed for the local and nonlocal detections of Figure 1.9a and b and also for the local detection of Figure 1.9d in which the channel does not extend outside the length L between the contacts (confined spin relaxation). The output signal, $\Delta R = (V_{AP} - V_P)/I$, is plotted as a function of the ratio of the mean interface resistance $R_T^\star$ (defined in the caption and supposed to be the same for the contacts F1 and F2) to the spin resistance of the channel (R_N = product of the resistivity by the SDL λ_N divided by the section; the spin relaxation per unit length of N is inversely proportional to R_N) for the three geometries of Figure 1.9a–d (other details on the parameters are in the caption of the figure). The calculation is performed in a situation of "conductivity mismatch," that is, $R_F \ll R_N$, so that, for the three curves, the spin signal turns out when $R_T^\star$ exceeds R_N. Then, the difference between the three curves illustrates an important rule: the scale of ΔR is the "resistance" controlling the spin relaxation. For a and b with $R_T^\star \gg R_N$, the relaxation in N between − and $+\lambda_N$ is larger ($\propto 1/R_N$) than the spin escape through $R_T^\star$ ($\propto 1R_T^\star$) and ΔR flattens out at a level of the order of $R_N \ll R_T^\star$ ($\approx 2\gamma^2 R_N \exp(-L/\lambda_N)$ for local detection and $\approx \gamma^2 R_N \exp(-L/\lambda_N)$ for nonlocal). In contrast for d with $R_N \ll R_T^\star \ll R_N \lambda_N / L$, the relaxation is controlled by the spin escape through $R_T^\star$ (rather than by the relaxation inside L) and ΔR goes on increasing in proportion of $R_T^\star$ well above the saturation value $\approx R_N$ of the open structures a and b. This regime, also described by a dwell time τ_n shorter than the spin lifetime τ_{sf}, is illustrated by the large MR observed in CNTs (60%–70%, ΔR in the MΩ range well above the spin resistance of the nanotube)

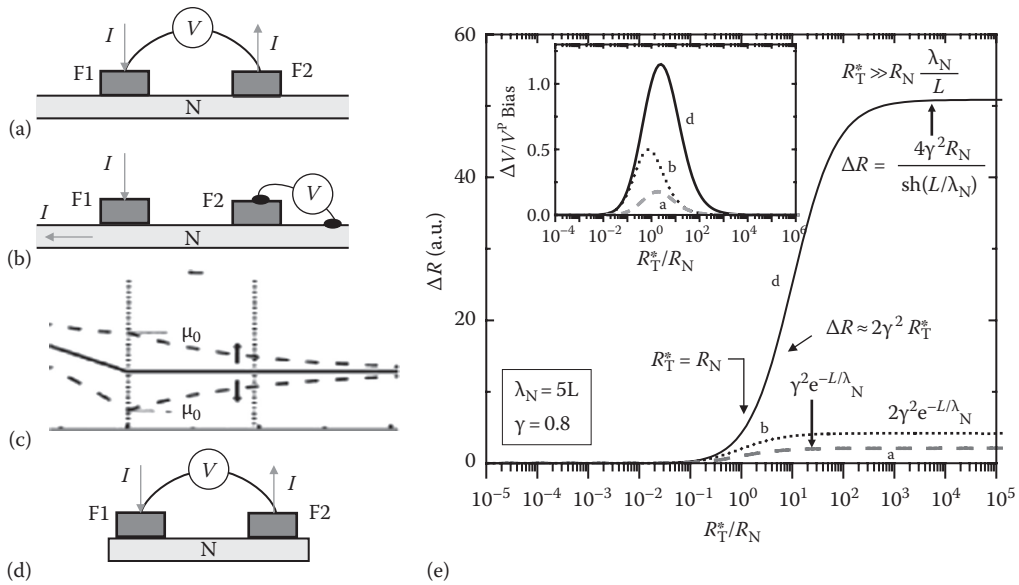

FIGURE 1.9 (a) and (b) Geometries for lateral spin transport between spin-polarized sources and drains with, respectively, local and nonlocal detection of the "spin signal." (c) Spin-up and spin-down electrochemical potential profiles for the nonlocal geometry of (b). The nonlocal signal V is related to the splitting (spin accumulation) under the nonlocal contact. (d) Geometry similar to (a) but with a lateral channel not extending outside the contacts. (e) Output spin signal, $\Delta R = [V_{AP} - V_P]/I$, for geometries of (a), (b), (d) calculated from drift/diffusion equations as a function of $R_T^\star/R_N$ with the following definitions: L = length between F1 and F2, $R_{T\uparrow(\downarrow)} = 2\,[1 - (+)\gamma]\,R_T^\star$ = tunnel resistances between the channel and F1 or F2, $R_N = \rho_N\lambda_N/S_N$ = channel spin resistance (ρ_N = resistivity, λ_N = SDL, S_N = section), $R_F = \rho_F^\star\lambda_F/S_F \ll R_N$ ($\gamma = 0.8$, $\lambda_N = 5L$ in the calculation). ΔR flattens out at a value of the order of R_N for $R_T^\star \gg R_N$ in the open structures of (a) and (b) (dotted and dashed lines). For the geometry of (d), ΔR does not flatten out for $R_T^\star > R_N$ and goes on increasing proportionally to $R_T^\star$ before reaching saturation at the level $4\gamma^2R_N/\mathrm{sh}(L/\lambda_N)$, well above R_N, for $R_T^\star \gg R_N\lambda_N/L$ (solid line).

[46]. Then, for $R_T^\star \gg R_N\lambda_N/L$, the relaxation inside L becomes predominant and ΔR flattens out at the level $4\gamma^2R_N/\mathrm{sh}(\lambda_N/L) \approx 4\gamma^2R_N\lambda_N/L$ (well above the saturation for curves a and b in Figure 1.9e). For confined relaxation with nonlocal detection $4\gamma^2R_N/\mathrm{sh}(L/\lambda_N)$ becomes $3\gamma^2R_N/\mathrm{sh}(L/\lambda_N)$, as shown by Jaffrès et al. [49]. The different rules described above can explain the main features of the results found in various structures with metals, semiconductor, or carbon-based materials.

In Figure 1.10, we show examples of lateral spin transport in the simple situation of a metallic channel and ohmic contacts with metallic electrodes [50,52,54,55]. The output signal ΔR, at the typical scale of the channel spin resistance, is typically of the order of a few mΩ, which corresponds to local or nonlocal output voltages in the μV range for current densities in the 10^7 A/cm^2 range (the ratio to the bias voltage can reach 10%). With a metallic channel but with tunnel contacts, most experiments have been performed in the geometry of Figure 1.9a and b, so that the output signals are larger but do not exceed significantly the spin resistance of a metallic channel ($\Delta R \approx 10^{-3} - 10^{-4}\,R_{bias}$). For the experiments with a semiconducting channel, generally performed with tunnel or Schottky contacts to solve the "conductivity mismatch," the review article of Jonker and Flatté [56] concludes that the contrast between the conductance of the parallel and antiparallel configuration never exceeds the range 0.1%–1%. With CNTs and tunnel contacts in the range of 100 MΩ with $La_{2/3}Sr_{1/3}MnO_3$ (LSMO) electrodes [46], some experiments in the geometry of Figure 1.9d have led to output signals $\Delta R \approx 90$ MΩ (60% of the total resistance of the two contacts), which appears to correspond to the situation of the corresponding curve in Figure 1.9e with $\Delta R \approx R_T \gg R_{CNT}$. This shows the possibility of obtaining large spin signals at the level of tunnel resistances by preventing the spin relaxation in branches of small spin resistance. This also reflects the potential of carbon-based materials like CNT [46,57] or graphene [58], which can combine a long spin lifetime, due to the small spin–orbit of carbon, with the advantage of their very high electron velocity for short dwell times.

1.8 Spin Transfer

Spin transfer gives means to manipulate the magnetic moment of a ferromagnetic body without applying any magnetic field but only by transfer of spin angular momentum from a spin-polarized current. The concept that has been introduced by Slonczewski [59] and appears also in papers of Berger [60] is illustrated in Figure 1.11. As described in the caption of the figure, the transfer of the transverse component of a spin current to the "free" magnetic layer F2 can be described by a torque acting on the magnetic moment of F2. This torque can induce a switching or reorientation of this magnetic moment, which can be described as a transport of nonvolatile magnetization by an electrical wire. In a second regime, generally in the presence of an applied field, the spin transfer torque generates periodic motions of the magnetic moment and voltage oscillations in the microwave frequency

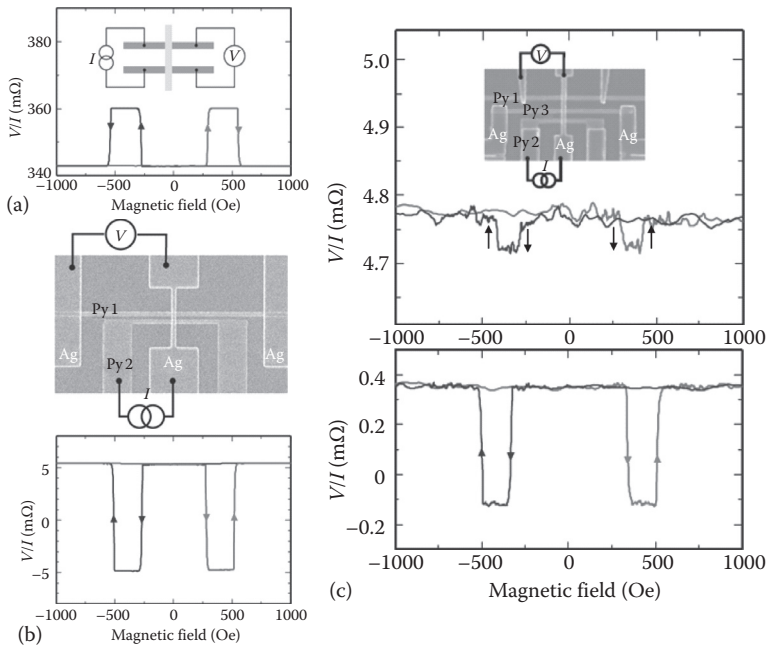

FIGURE 1.10 Experimental examples of lateral spin transport in permalloy/silver nanodevices [55]. (a) Local spin-valve measurements at 77 K. A sketch of the nanodevice is shown above the experimental curves. (b) Nonlocal spin-valve measurements at 77 K. An image of the nanodevice is shown on the top. (c) Nonlocal spin-valve measurements at 77 K (bottom) and room temperature (middle) on a nanodevices similar to that of (b) but with an additional permalloy contact (Py3 on the image) between the injection and detection contacts. The signal reduction with respect to devices without additional contact is due to the spin current escaping through this contact and relaxing in the additional channel. The reduction is inversely proportional to the spin resistance of the additional channel and, for example, becomes larger and larger as one goes from Cu to Au and Py. (From Kimura, T. et al., *Phys. Rev. B*, 72, 014461-1–6, 2005. With permission.)

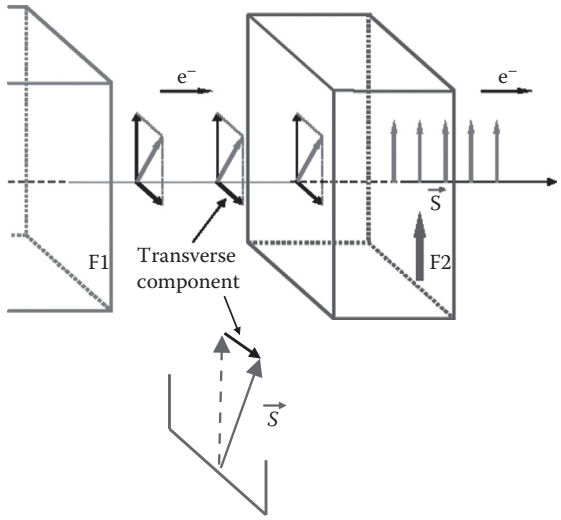

FIGURE 1.11 Illustration of the spin transfer concept introduced by Slonczewski [59]. A spin-polarized current is prepared by a first magnetic layer F with an obliquely oriented spin polarization with respect to the magnetization axis of a second layer F2. When it goes through F2, the exchange interaction aligns its spin polarization along the magnetization axis. The exchange interaction being spin conserving, the transverse spin polarization lost by the current is transferred to the total spin of F2, which can also be described by a spin-transfer torque acting on F2. (From Chappert, C. et al., *Nat. Mater.*, 6, 813, 2007. With permission.)

range. Actually the concept of spin transfer has opened a new face of spintronics: GMR or TMR allowed us to detect electrically a magnetic configuration, while spin transfer now enables us to create a magnetic configuration with an electrical current.

The first evidence that spin transfer can work was indicated by experiments of spin injection through point contacts by Tsoi et al. [61], but a clear understanding came later from measurements [63,64] performed on pillar-shaped metallic trilayers and tunnel junctions (Figure 1.12a), or by injecting a current into a magnetic trilayer through the type of nanocontact represented in Figure 1.12b [64]. In Figure 1.12c, we show an example of magnetic switching detected by GMR in a metallic pillar. Figure 1.12d represents the microwave power spectrum of the voltage oscillations generated by current-induced magnetic precessions in a structure of nanocontact type. Actually the spin transfer torque can be used not only to induce switchings and precessions of magnetic moments but also more sophisticated magnetic excitations. Figure 1.12e shows the microwave power spectrum generated by the gyration of the core of a magnetic vortex in one of the electrodes of an MTJ [65]. Alternatively, the spin transfer torque can also be used to move domain walls in nanowires. These many very different spin transfer experiments raise a great variety of interesting physical problems mixing spin transport, spin dynamics, and micromagnetism.

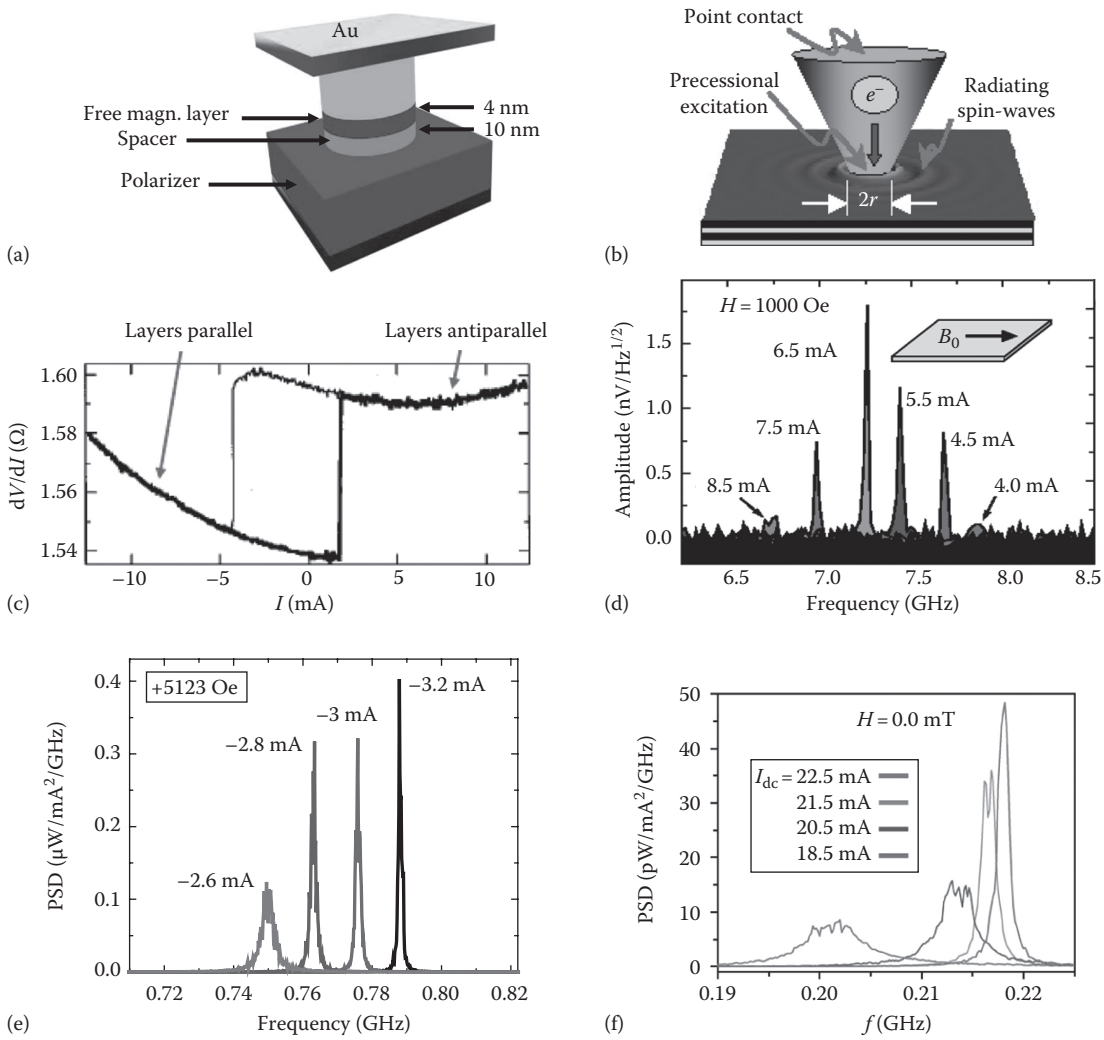

FIGURE 1.12 (See color insert.) (a) and (b) Nanodevices for spin transfer experiments ("pillar" and nanocontacts [64]). (c) Differential resistance vs. current for a Co/Cu/Co "pillar" with current-induced switchings between parallel and antiparallel magnetic configurations [62]. (d) Microwave spectra obtained by current injection into a CoFe/Cu/NiFe trilayer through a nanocontact at different values of current [64]. (e) Microwave power spectra obtained at different values of current from vortex gyrations in the permalloy layer of a CoFeB/MgO/Permalloy MTJ [65]. (f) Progressive synchronization of the gyration of four vortices appearing at increasing current in the microwave spectrum of a device for current injection into a Co/Cu/permalloy trilayer through four nanocontacts. (From Ruotolo, A. et al., *Nat. Nanotechnol.*, 4, 528, 2009. With permission.)

The spin transfer phenomena will have certainly important applications. Switching by spin transfer will be used in the next generation of MRAMs (called STT-RAMs) for a more precise addressing and a smaller energy consumption. The generation of oscillations in the microwave frequency range will lead to the design of spin transfer oscillators (STOs). One of the main interests of the STOs is their tunability, that is the possibility of changing rapidly their frequency by tuning a DC current. Their disadvantage is the very small microwave power of an individual STO. The microwave power obtained with MTJs is not too far from what is needed for applied devices but the linewidth of their emission is still much too broad. Today it seems that the excitation of magnetic vortices in MTJs heads the race on the way to application as they combine power and narrow linewidth see Figure 1.12e [65]. An interesting challenge, to increase the emitted power and reduce the linewidth, is the synchronization of a set of STOs. Figure 1.12f shows an example of synchronization of the gyration of a square of four vortices [66].

1.9 Spintronics Today and Tomorrow

Nowadays spintronics is expanding in so many directions that we will only list and summarize the main axes.

The very active research [67] on the axis "spintronics with semiconductors" aims at combining the potential of semiconductors (control of current by gate, coupling with optics, etc.) with the potential of the magnetic materials (control of current by spin manipulation, non-volatility, etc.). It should be possible,

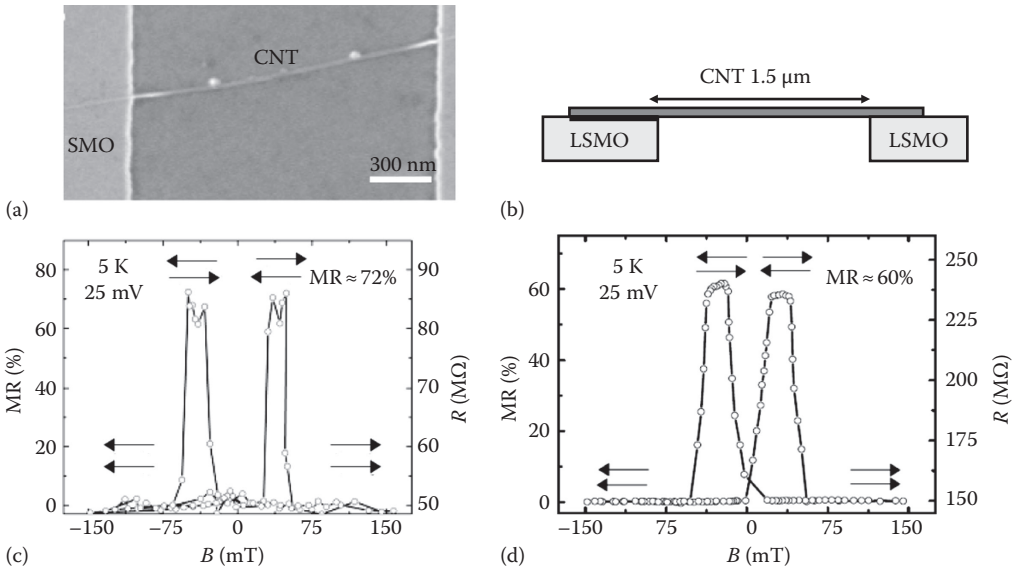

FIGURE 1.13 Spin transport through carbon nanotubes (CNTs) [46]. (a) Electron microscope image of a CNT between LSMO electrodes. (b) Schematic side view of the device. (c), (d) Examples of MR experimental results. The resistance R of the device is predominantly due to the tunnel resistance at the LSMO/CNT interfaces, and its change between the parallel and antiparallel magnetic configuration is about 72% (c) or 60% (d).

for example, to gather storage, detection, logic, and communication capabilities on a single chip that could replace several components. One of the ways is with ferromagnetic semiconductors (FSs) based on the well-known semiconductors of today. Excellent results have been obtained with GaAs doped wit Mn [68], but it has not been possible to increase its Curie temperature above 170 K and this rules out most possibilities of applied devices. Some announcements of FS at room temperature have been made, but the situation is still rather confused on this point today. The second way is the fabrication of hybrid structures associating ferromagnetic metals and conventional semiconductors. In a spin LED [69–72], for example, the injection of spin-polarized current into an LED leads to the emission of a circularly polarized light. In other experiments, it has been now possible to detect electrically the spin accumulation injected into a semiconductor [72–75]. An intense research has been devoted to the implementation of the concept of spin transistor proposed by Datta and Das [76], but only very modest advances [77] have been made on this topic up to now. Finally, a hot topic of today is the SHE and the QSHE [78,79].

Spintronics with multiferroics is also a promising axis. Multiferroic materials combine ferromagnetic and ferroelectric properties, and the possible coupling between the ferromagnetic and ferroelectric orders could give means to control a magnetic configuration with an electric field [80–82]. The recent results [82] with $BiFeO_3$ are promising, and the research on several other types of multiferroic oxides is now very active. Note that an alternative way for an electric field control of the magnetization direction turns out to be through direct effects on the band structure by spin–orbit interactions in FSs [83] or even in ultrathin layers of ferromagnetic metals [84].

Other interesting new properties of oxides have been revealed recently. For example, the existence of 2DEGs of high mobility at the interface between two insulating oxides [85–87] opens the way to spintronic devices exploiting these 2DEGs in "all oxide" nanostructures. Also the extension of the technologies developed for MTJ to tunnel junctions with ferroelectric barriers has led to the observation of huge electroresistance effects [88] and to interesting prospects for the design of ferroelectric memories.

Another important field of research today is spintronics with carbon-based materials. Their general advantage comes from the long spin lifetime related to the small spin–orbit coupling of carbon. For metallic CNT and graphene, another advantage comes from their linear dispersion curves and very large velocities even for small carrier concentrations. In lateral spin-valve structures of CNT between LSMO electrodes (Figure 1.13), the MR can reach 60%–70% ($V_{AP} - V_P \approx 60$ mV for $V_P \approx 100$ mV for the sample of Figure 1.13d), well above the output electrical signals that can be obtained with semiconductor lateral channels. These results can be explained not only by the long spin lifetime in CNT but also by the short dwell time resulting from the high velocity of the electrons inside CNTs [46]. Promising experimental results with graphene and various molecules have been also recently published [58,89,90].

Finally, with qbits based on the spin state of a quantum box, nanospintronics is one of the ways to quantum computing. This is certainly one of the most exiting perspectives, out of the scope of this chapter, and, on this point, we refer to a recent review by Trauzettel et al. [91].

1.10 Conclusion

In about 20 years, we have seen spintronics increasing considerably the capacity of our hard discs, extending the hard disc

technology to mobile appliances like cameras or portable multimedia players, entering the automotive industry and the biomedical technology and, with TMR and spin transfer, getting ready to enter the RAM of our computers or the microwave emitters of our cell phones. The researches of today on the spin transfer phenomena, on multiferroic materials, on spintronics with semiconductors and molecular spintronics, open fascinating new fields and are also very promising in the "beyond CMOS" perspective. Spintronics is still a young baby in the science family, but this baby is growing remarkably well.

References

1. M. N. Baibich, J. M. Broto, A. Fert et al., Giant magnetoresistance of (001) Fe/(001) Cr magnetic superlattices, *Phys. Rev. Lett*. **61**, 2472–2475 (1988).
2. G. Binash, P. Grünberg, F. Saurenbach et al., Enhanced magnetoresistance in layered magnetic structures with antiferromagnetic interlayer exchange, *Phys. Rev. B* **39**, 4828–4830 (1989).
3. N. F. Mott, The electrical conductivity of transition metals, *Proc. Roy. Soc. A* **153**, 699–718 (1936).
4. A. Fert and I. A. Campbell, Two current conduction in nickel, *Phys. Rev. Lett*. **21**, 1190–1192 (1968); A. Fert and I. A. Campbell, Transport properties of ferromagnetic transition metals, *J. Phys*. **32**, C1–46–50 (1971); A. Fert and I. A. Campbell, Electrical resistivity of ferromagnetic nickel and iron based alloys, *J. Phys. F Met. Phys*. **6**, 849–871 (1976).
5. B. Loegel and F. Gautier, Origine de la résistivité dans le cobalt et ses alliages dilués, *J. Phys. Chem. Sol*. **32**, 2723–2735 (1971).
6. J. Barnas, O. Baksalary, and Y. Bruynseraede, Effect of interchannel transitions in the current-in-plane giant magnetoresistance, *J. Phys.: Condens. Matter* **7**, 6437–6448 (1995).
7. A. Fert, A. Barthélémy, and F. Petroff, Spin transport in magnetic multilayers and tunnel junctions, in *Nanomagnetism: Ultrathin Films and Nanostructures*, F. Mills and J. A. C. Bland (Eds.), Elsevier, Amsterdam, the Netherlands, pp. 153–226, 2006.
8. M. I. D'yakonov and V. I. Perel', Possibility of orienting electron spins with current, *JETP Lett*. **13**, 467–469 (1971).
9. L. Vila, T. Kjimura, and Y. Otani, Evolution of the spin Hall effect in Pt nanowires: Size and temperature effects, *Phys. Rev. Lett*. **99**, 226604-1–4 (2007).
10. S. O. Valenzuela and M. Tinkham, Direct measurement of the spin Hall effect, *Nature* **442**, 176–179 (2006).
11. T. Seki, Y. Hasegawa, S. Mitani et al., Giant spin Hall effect in perpendicularly spin-polarized FePt/Au devices, *Nat. Mater*. **7**, 125–128 (2008).
12. A. Fert, A. Friederich, and A. Hamzic, Hall effect in dilute magnetic alloys, *J. Magn. Magn. Mater*. **24**, 231–257 (1981).
13. Y. K. Kato, R. C. Myers, A. C. Gossard et al., Observation of the spin Hall effect in Semiconductors, *Science* **306**, 1910–1913 (2004).
14. P. Grünberg, R. Schreiber, Y. Young et al., Layered magnetic structures: Evidence for antiferromagnetic coupling of Fe layers across Cr interlayers, *Phys. Rev. Lett*. **57**, 2442–2445 (1986).
15. R. E. Camley and J. Barnas, Theory of giant magnetoresistance effects in magnetic layered structures with antiferromagnetic coupling, *Phys. Rev. Lett*. **63**, 664–667 (1989).
16. P. M. Levy, S. Zhang, and A. Fert, Electrical conductivity of magnetic multilayered structures, *Phys. Rev. Lett*. **65**, 1643–1646 (1990).
17. S. S. P. Parkin, N. More, and K. P. Roche, Oscillations in exchange coupling and magnetoresistance in metallic superlattice structure: Co/Ru, Co/Cr, and Fe/Cr, *Phys. Rev. Lett*. **64**, 2304–2307 (1990).
18. T. Shinjo and H. Yamamoto, Large magnetoresistance of field-induced giant ferromagnetic multilayers, *J. Phys. Soc. Jpn*. **59**, 3061–3064 (1990).
19. C. Dupas, P. Beauvillain, C. Chappert et al., Very large magnetoresistance effects induced by antiparallel magnetization in two ultrathin cobalt films, *J. Appl. Phys*. **67**, 5680–5682 (1990).
20. D. H. Mosca, F. Petroff, A. Fert et al., Oscillatory interlayer coupling and giant magnetoresistance in Co/Cu multilayers, *J. Magn. Magn. Mater*. **94**, L1–L5 (1991).
21. S. S. P. Parkin, R. Bhadra, and K. P. Roche, Oscillatory magnetic exchange coupling through thin copper layers, *Phys. Rev. Lett*. **66**, 2152–2155 (1991).
22. B. Dieny, V. S. Speriosu, S. S. P. Parkin et al., Giant magnetoresistance in soft ferromagnetic multilayers, *Phys. Rev. B* **43**, 1297–1300 (1991).
23. S. S. P. Parkin, Applications of magnetic nanostructures, in *Spin Dependent Transport in Magnetic Nanostructures*, S. Maekawa and T. Shinjo (Eds.), Taylor & Francis, London, pp. 237–279, 2002.
24. C. Chappert, A. Fert, and F. Nguyen Van Dau, The emergence of spin electronics in data storage, *Nat. Mater*. **6**, 813–823 (2007).
25. P. P. Freitas, H. Ferreira, D. Graham et al., Magnetoresistive biochips, *Europhys. News* **34/6**, 224–226 (2003).
26. M. Jullière, Tunneling between ferromagnetic films, *Phys. Lett. A* **54**, 225–226 (1975).
27. S. Maekawa and O. Gäfvert, Electron tunneling between ferromagnetic films, *IEEE Trans. Magn. MAG* **18**, 707–708 (1982).
28. J. S. Moodera, L. R. Kinder, T. M. Wong et al., Large magnetoresistance at room temperature in ferromagnetic thin film tunnel junctions, *Phys. Rev. Lett*. 74, 3273–3276 (1995); T. Miyazaki and N. Tezuka, Giant magnetic tunneling effect in Fe/Al_2O_3/Fe junction, *J. Magn. Magn. Mater*. **139**, L231–L234 (1995).
29. M. Bowen, V. Cros, F. Petroff et al., Large magnetoresistance in Fe/MgO/FeCo(001) epitaxial tunnel junctions on GaAs(001), *Appl. Phys. Lett*. **79**, 1655–1657 (2001).
30. S. Yuasa, T. Nagahama, K. Fukushima et al., Giant room-temperature magnetoresistance in single-crystal Fe/MgO/Fe magnetic tunnel junctions, *Nat. Mater*. **3**, 868–871 (2004).

31. S. S. P. Parkin, C. Kaiser, A. Panchula et al., Giant tunneling magnetoresistance at room temperature with MgO(100) tunnel barriers, *Nat. Mater*. **3**, 862–867 (2004).
32. Y. M. Lee, J. Hayakawa, S. Ikeda et al., Effect of electrode composition on the tunnel magnetoresistance of pseudo-spin-valve magnetic tunnel junction with a MgO tunnel barrier, *Appl. Phys. Lett*. **90**, 212507-1–3 (2007).
33. L. Jiang, H. Naganuma, M. Oogane et al., Large tunnel magnetoresistance of 1056% at room temperature in MgO based double barrier magnetic tunnel junctions, *Appl. Phys. Express* **2**, 083002-1–3 (2009).
34. I. I.Oleinik, E. Y. Tsymbal, and D. G. Pettifor, Structural and electronic properties of $CoAl_2O_3$/Co magnetic tunnel junction from first principles, *Phys. Rev. B* **62**, 3952–3959 (2000); I. I. Oleinik, E. Y. Tsymbal, and D. G. Pettifor, Atomic and electronic structure of Co/$SrTiO_3$/Co magnetic tunnel junctions, *Phys. Rev. B* **65**, 020401-1–4 (2002).
35. J. Mathon and A. Umerski, Theory of tunneling magnetoresistance in a junction with a nonmagnetic metallic interlayer, *Phys. Rev. B* **60**, 1117–1121 (1999).
36. Ph. Mavropoulos, N. Papanikolaou, and P. H. Dederichs, Complex band structure and tunneling through ferromagnet/insulator/ferromagnet junctions, *Phys. Rev. Lett*. **85**, 1088–1091 (2000).
37. X.-G. Zhang and W. H. Butler, Large magnetoresistance in bcc Co/MgO/Co and FeCo/MgO/FeCo tunnel junctions, *Phys. Rev. B* **70**, 173407-1–4 (2004).
38. J. P. Velev, K. D. Belashchenko, D. A. Stewart et al., Negative spin polarization and large tunneling magnetoresistance in epitaxial Co/$SrTiO_3$/Co magnetic tunnel junctions, *Phys. Rev. Lett*. **95**, 216601-1–4 (2005).
39. J. M. De Teresa, A. Barthélémy, A. Fert et al., Role of metal-oxide interface in determining the spin polarization of magnetic tunnel junctions, *Science* **286**, 507–509 (1999).
40. M. Bowen, M. Bibes, A. Barthélémy et al., Nearly total spin polarization in $La_{2/3}Sr_{1/3}MnO_3$ from tunneling experiments, *Appl. Phys. Lett*. **82**, 233–235 (2003).
41. T. Ishikawa, T. Marukame, H. Kijima et al., Spin-dependent tunneling characteristics of fully epitaxial magnetic tunneling junctions with a full-Heusler alloy Co_2MnSi thin film and a MgO tunnel barrier, *Appl. Phys. Lett*. **89**, 192505-1–3 (2006).
42. P. LeClair, J. K. Ha, J. M. Swagten et al., Large magnetoresistance using hybrid spin filter devices, *Appl. Phys. Lett*. **80**, 625–627 (2002).
43. W. P. Pratt, S. F. Lee, J. M. Slaughter et al., Perpendicular giant magnetoresistances of Ag/Co multilayers, *Phys. Rev. Lett*. **66**, 3060–3063 (1991); J. Bass and W. P. Pratt, Jr., Current-perpendicular (CPP) magnetoresistance in magnetic metallic multilayers, *J. Magn. Magn. Mater*. **200**, 274–289 (1999).
44. L. Piraux, J.-M. George, C. Leroy et al., Giant magnetoresistance in magnetic multilayered nanowires, *Appl. Phys. Lett*. **65**, 2484–2486 (1994); A. Fert and L. Piraux, Magnetic nanowires, *J. Magn. Magn. Mater*. **200**, 338–358 (1999).
45. T. Valet and A. Fert, Theory of the perpendicular magnetoresistance in magnetic multilayers, *Phys. Rev. B* **48**, 7099–7013 (1993).
46. L. E. Hueso, J. M. Pruneda, V. Ferrari et al., Transformation of spin information into large electrical signals using carbon nanotubes, *Nature* **445**, 410–413 (2007).
47. G. Schmidt, D. Ferrand, L. W. Molenkamp et al., Fundamental obstacle for electrical spin injection from a ferromagnetic metal into a diffusive semiconductor, *Phys. Rev. B* **62**, 4790–4793 (2000).
48. E. I. Rashba, Theory of electrical spin injection: Tunnel contacts as a solution of the conductivity mismatch problem, *Phys. Rev. B* **62**, R16267–R1670 (2000).
49. A. Fert and H. Jaffrès, Conditions for efficient spin injection from a ferromagnetic metal into a semiconductor, *Phys. Rev. B* **64**, 184420-1–9 (2001); A. Fert, J.-M. George, H. Jaffrès, and R. Mattana, Semiconductors between spin-polarized sources and drains, *IEEE Trans. Electron Dev*. **54**, 921–932 (2007); H. Jaffrès, A. Fert, and J.-M. George, *Phys. Rev. B*. 67, 140408(R), 8–11 (2010).
50. M. Johnson and R. H. Silsbee, Thermodynamic analysis of interfacial transport and of the thermomagnetoelectric system, *Phys. Rev. B* **35**, 4959–4972 (1987).
51. Z. G. Yu and M. E. Flatté, Electric-field dependent spin diffusion and spin injection into semiconductors, *Phys. Rev. B* **66**, 201202-1–4 (2002).
52. T. Kimura, J. Hamrle, and Y. Otani, Estimation of spin-diffusion length from the magnitude of spin-current absorption: Multi-terminal ferromagnetic/non-ferromagnetic hybrid structures, *Phys. Rev. B* **72**, 014461-1–6 (2005).
53. S. Takahashi and S. Maekawa, Spin currents in metals and superconductors, *J. Phys. Soc. Jpn*. **77**, 031009-1–14 (2008).
54. F. J. Jedema, M. S. Nijboer, A. T. Filip et al., Spin injection and spin accumulation in all-metal mesoscopic spin valves, *Phys. Rev. B* **67**, 085319-1–16 (2003).
55. T. Kimura and Y. Otani, Large spin accumulation in a permalloy-silver lateral spin valve, *Phys. Rev. Lett*. **99**, 196604 (2007).
56. B. T. Jonker and M. E. Flatté, Electrical spin injection and transport in semiconductors, in *Nanomagnetism: Ultrathin Films, Multilayers and Nanostructures*, D. L. Mills and J. A. C. Bland (Eds.), Elsevier, Amsterdam, pp. 227–272, 2006.
57. A. Cottet, T. Kontos, S. Sahooo et al., Nanospintronics with carbon nanotubes, *Semicond. Sci. Technol*. **21**, S78–S95 (2006).
58. N. Tombros, C. Jozsa, M. Popinciuc et al., Electronic transport and spin precession in single graphene layers at room temperature. *Nature* **448**, 571–574 (2006); M. Ohishi, M. Shiraishi, R. Nouchi et al., Spin injection into graphene at room temperature, *Jpn. J. Appl. Phys*. **46**, 25–28 (2007); W. Han, K. Pi, K. McCreary et al., Tunneling spin injection into single layer graphene, *Phys. Rev. Lett*. **105**, 16702–16704 (2010).
59. J. C. Slonczewski, Current-driven excitation of magnetic multilayers, *J. Magn. Magn. Mater*. **159**, L1–L7 (1996).
60. L. Berger, Emission of spin waves by a magnetic multilayer traversed by a current, *Phys. Rev. B* **54**, 9353–9358 (1996).

61. M. Tsoi, A. G. M. Jansen, J. Bass et al., Excitation of a magnetic multilayer by an electric current, *Phys. Rev. Lett*. **80**, 4281–4284 (1998).
62. F. J. Albert, J. A. Katine, F. J. Albert et al., Spin-polarized current switching of a Co thin film nanomagnet, *Appl. Phys. Lett*. **77**, 3809–3811 (2000).
63. J. Grollier, V. Cros, A. Hamzic et al., Spin-polarized current induced switching in Co/Cu/Co pillars, *Appl. Phys. Lett*. **78**, 3663–3665 (2001).
64. W. H. Rippart, M. R. Pufall, S. Kaka et al., Direct-current induced dynamics in $Co_{90}Fe_{10}/Ni_{80}Fe_{20}$ point contacts, *Phys. Rev. Lett*. **92**, 027201-1–4 (2004).
65. A. Dussaux, B. Georges, J. Grollier et al., Large microwave generation from current-driven magnetic vortex oscillators in magnetic tunnel junctions, *Nat. Commun*. (2010) DOI:10.1038/ncommas1006.
66. A. Ruotolo V. Cros, B. Georges et al., Spin transfer induced dynamics of an array of interacting vortices in a periodic potential, *Nat. Nanotechnol*. **4**, 528–532 (2009).
67. I. Žutić, J. Fabian, and S. Das Sarma, Spintronics: Fundamentals and applications, *Rev. Mod. Phys*. **76**, 323–410 (2004).
68. H. Ohno, A. Shen, and F. Matsukura, (Ga,Mn)As: A new diluted magnetic semiconductor based on GaAs, *Appl. Phys. Lett*. **69**, 363–365 (1996).
69. V. F. Motsnyi, P. Van Dorpe, W. Van Roy et al., Optical investigation of spin injection into semiconductors, *Phys. Rev. B* **68**, 245319 (2003).
70. A. T. Hanbicki, M. J. van't Erve, and R. Magno, Analysis of the transport process providing spin injection through an Fe/AlGaAS Schottky barrier, *Appl. Phys. Lett*. **82**, 4092–4094 (2003).
71. Y. Lu, V. G. Truong, P. Renucci et al., MgO thickness dependence of spin injection efficiency in spin-light emitting diodes, *Appl. Phys. Lett*. **93**, 152102-1–3 (2008).
72. X. Lou, C. Adelmann, S. A. Crooker et al., Electrical detection of spin transport in lateral ferromagnet–semiconductor devices, *Nat. Phys*. **3**, 197–202 (2007).
73. O. Van't Erve, A. T. Hanbicki, M. Holub et al., Electrical injection and detection of spin-polarized carriers in silicon in a lateral transport geometry, *Appl. Phys. Lett*. **91**, 212109-1–3 (2007).
74. M. Tran, H. Jaffrès, C. Deranlot et al., Enhancement of the spin accumulation at the interface between a spin-polarized tunnel junction and a semiconductor, *Phys. Rev. Lett*. **102**, 036601-1–4 (2009).
75. S. P. Dash, S. Sharma, R. S. Pald et al., Electrical creation of spin polarization in silicon at room temperature, *Nature* **462**, 491–494 (2009).
76. S. Datta and B. Das, Electronic analog of the electro-optic modulator, *Appl. Phys. Lett*. **56**, 665–667 (1990).
77. H.-C. Koo, J.-H. Kwon, J. Eom et al., Control of spin precession in a spin-injected field effect transistor, *Science* **325**, 1515–1518 (2009).
78. M. König, S. Wiedmann, and C. Brüne, Quantum spin Hall insulator state in HgTe quantum wells, *Science* **318**, 766–770 (2007).
79. D. Hsieh, Y. Xia, D. Qian et al., Observation of time-reversal-protected single-Dirac-Cone topological-insulator states in Bi_2Te_3 and Sb_2Te_3, *Phys. Rev. Lett*. **103**, 146401-1–4 (2009).
80. T. Zhao, A. Scholl, F. Zavaliche et al., Electrical control of antiferromagnetic domains in multiferroic $BiFeO_3$ films at room temperature, *Nat. Mater*. **5**, 823–829 (2006); H. Béa, M. Bibes, F. Ott et al., Mechanisms of exchange bias with multiferroic $BiFeO_3$ epitaxial films, *Phys. Rev. Lett*. **100**, 017204 (2008); J. D. Burton and E. Y. Tsymbal, Prediction of electrically induced magnetic reconstruction at the manganite/ferroelectric interface, *Phys. Rev. B* **80**, 1744061–1744065 (2009).
81. M. Bibes and A. Barthélémy, Oxide spintronics, *IEEE Trans. Electron. Dev*. **54**, 1003–1023 (2007).
82. Y.-H. Chu, L. W. Martin, M. B. Holcomb et al., Electric-field control of local ferromagnetism using a magnetoelectric multiferroic, *Nat. Mater*. **7**, 478–482 (2008).
83. D. Chiba, M. Sawicki, Y. Nishitami et al., Magnetization vector manipulation by electric field, *Nature* **455**, 515–518 (2008).
84. M. Weisheit, S. Fähler, A. Marty et al., Electric field-induced modification of magnetization in thin-film ferromagnets, *Science* **315**, 349 (2007).
85. A. Ohtomo and H. Y. Hwang, A high-mobility electron gas at the $LaAlO_3/SrTiO_3$ heterointerface, *Nature* **427**, 423–426 (2004).
86. M. Basletic, J.-L. Maurice, C. Carrétéro et al., Mapping the spatial distribution of charge carriers in $LaAlO_3/SrTiO_3$ heterostructures, *Nat. Mater*. **7**, 621–25 (2008); C. Cen, S. Thiel, J. Mannhart et al., Oxide nanoelectronics on demand, *Science* **323**, 1026–1028 (2009).
87. M. K. Niranjan, Y. Wang, S. S. Jaswal et al., Prediction of a switchable two-dimensional electron gas at ferroelectric oxide interfaces, *Phys. Rev. Lett*. **103**, 016804-1–4 (2009).
88. V. Garcia, S. Fusil, K. Bouzehouane et al., Giant tunnel electroresistance for non-destructive readout of ferroelectric states, *Nature* **460**, 81–84 (2009).
89. Z. H. Xiong, D. Wu, V. Vardeny et al., Giant magnetoresistance in organic spin-valves, *Nature* **427**, 821–824 (2004).
90. W. J. M. Naber, S. Faez, and W. G. Van der Wiel, Organic spintronics, *J. Phys. D: Appl. Phys*. **40**, R205–R228 (2007).
91. B. Trauzettel, M. Borhani, M. Trif et al., Theory of spin qubits in nanostructures, *J. Phys. Soc. Jpn*. **77**, 031012 (2008).